SUPERSONIC DIFFUSER INSTABILITY

Thesis by

Charles Lee Dailey

In Partial Fulfillment of the Requirements

for the Degree of

Doctor of Philosophy

California Institute of Technology

Pasadena, California

1954

ACKNOWLEDGMENTS

The author wishes to express his appreciation to Mr. P. O. Johnson for his many valuable suggestions concerning the analysis and interpretation of the experimental data. He also wishes to express his gratitude to Drs. H. W. Liepmann, H. J. Stewart, H. S. Tsien, and F. Marble for their helpful discussions.

Permission by the Bureau of Aeronautics to publish the data presented herein is greatly appreciated. In addition, the author expresses his gratitude to the California Institute of Technology and to the University of Southern California Engineering Center for their cooperative assistance in making possible the preparation of this thesis.

SUMMARY

Steady operation of supersonic diffusers near critical mass flow is interrupted by a transient process known as buzz. This phenomenon consists of a random sequence of individual relaxation cycles. Mass flow entering the diffuser during steady operation is suddenly cut off by a strong interaction between the subcritical shock and boundary layer on the surface of the external compression generator, which blocks the inlet. Air in the plenum chamber, stored at high pressure, then "blows down" until the inlet can re-start. The subsequent supercritical flow entering the diffuser exceeds the flow rate at the exit and the plenum chamber is re-charged to the original condition.

A distinction is drawn between this phenomenon and a high frequency wave-type resonance noticed at low mass flows and during an individual buzz cycle after the diffuser shock system has been expelled. For the large diffuser tested here, this high frequency oscillation compares well to the 8th closed-end organ pipe mode of the diffuser at low mass flows and to the 9th mode during the shock-expelled phase of the buzz cycle.

It is shown that burning almost always ceases in the presence of buzz. When burning was maintained during buzz, it was found to have no qualitative effect on the buzz cycle.

TABLE OF CONTENTS

TABLE OF FIGURES

SYMBOLS

P	Pressure
ρ	Density
T	Temperature
γ	Ratio of specific heats
R	Gas constant
M	Mach number
R_N	Reynolds number
m	Mass flow rate
a	Speed of sound
t	Time
S	Cross-section area of stream tube
V	Total internal volume of diffuser model
ℓ	Effective length --- ratio of internal volume to plenum chamber cross-section area
F/A	Fuel to air ratio for combustion tests

Subscripts

0	Free stream conditions
1	Entrance to subsonic diffuser
2	End of subsonic diffuser
3	Station just downstream of flame arrester
4	End of combustion chamber
5	Sonic Station in exit nozzle
6	Station at engine exit

*	Local sonic conditions
s	Local stagnation conditions
c	Denotes critical diffuser mass flow
e	Engine exit

INTRODUCTION

There are two principal requirements of a supersonic diffuser: First, it must decelerate the entering air mass sufficiently to allow steady combustion, and second, it must compress the air mass before heat addition to achieve good thermal efficiency.

The former requirement is easily met; it is a simple matter to reduce the velocity approaching the burner to an arbitrarily low value by appropriate subsonic diffusion. The only penalty is a corresponding reduction in thrust relative to the burner frontal area. This is offset by an increase in cycle efficiency, but the gain is so small it is of no practical importance. In practice, every effort is made to achieve the maximum burner velocity compatible with good combustion efficiency and stable burner performance. Whatever this maximum is, it simply becomes a design requirement for the diffuser which can easily be met.

The latter problem is more complicated. In order to compress supersonic flow it is necessary to reduce the area through which it passes. In order to achieve good overall efficiency it is essential to obtain the maximum possible supersonic compression. This is obtained with the least inlet contraction ratio which will start. For fixed geometry diffusers, this requires the use of a central body to compress the flow before it enters the inlet. Diffusers without central bodies, or other means of external compression, are restricted so seriously by the starting problem that they are of no practical use at high Mach numbers. Unfortunately, however, the compression produced by the central body is accompanied by a cowl drag. Since both drag and efficiency increase directly with flow deflection, it is necessary to optimize the diffuser design in terms of net

thrust. Although this is somewhat more trouble than designing for a given burner velocity, it can be handled in a straightforward manner with existing methods.

An important feature of all supersonic diffusers is the existence of the supercritical regime which occurs when the inlet volume flow is a maximum for a given Mach number. The 'critical' point is simply the point of maximum compression efficiency in the supercritical regime, and is the condition for maximum net thrust of a ramjet. Operation of a ramjet at the critical point is achieved by increasing heat addition in the burner until the shock system within the engine is moved upstream to the inlet. The shock losses within the diffuser are thus minimized and the plenum chamber pressure is a maximum for supercritical operation. If further heat addition is attempted after this point has been reached, the diffuser enters the 'subcritical' regime and either one of two possible situations results. Either the flow remains steady, or flow breakdown occurs followed by a non-periodic fill-up and discharge of the plenum chamber known as 'buzz'.

From a practical standpoint it is obviously important to know when this instability might occur, so that operation under these conditions can be avoided. It is the purpose of the present investigation to determine the nature and cause of this instability.

It should be observed that different kinds of transient flow processes may occur in ducts, or internal flow systems in general. Depending on the duct geometry and flow conditions, these phenomena are sometimes even qualitatively different. It would be unrealistic to expect a mechanism which accounts for instability in one case to apply to all instances of internal flow system instability. For example, it would not be ex-

pected that the well known phenomena of compressor surge and the alternate stalling and unstalling of parallel ducts feeding the same plenum chamber could be explained by the same mechanism; nor would it be expected that axially symmetric supersonic diffusers with and without central bodies, or scoop diffusers, would necessarily exhibit the same transient flow characteristics. In fact, it should not even be supposed that geometrically similar diffusers operating at the same Mach number and Reynolds number, but with a significantly different scale factor, would behave the same; and it would certainly not be expected that the mechanism would, for a given case, be independent of mass flow.

It is therefore emphasized that this investigation deals principally with the problem of determining the cause and nature of the instability which has been observed to occur in axially symmetric diffusers, with central bodies, operating at high subcritical mass flows. It is the occurrence of this instability which defines the lower limit of steady subcritical operation for such a diffuser.

The first mention of this phenomenon in the literature appears in Reference 1. This is an NACA translation of a German report by Oswatitsch describing experimental work performed by him in 1942. Although his experiments were conducted with a small model (a few inches in length), and therefore did not have transient processes indicative of full scale engines, it is believed the mechanism leading to transition from steady flow to transient operation is the same as that which would occur at full scale.

Oswatitsch did not discuss the phenomenon in detail, but merely observed its occurrence. In fact, he dismissed the subject with the remark that it was unimportant since the subcritical range was impractical

anyway; an observation which is hardly realistic when one realizes that a sudden burst of instability could result in the failure of a supersonic ramjet missile or destruction of a high Mach number turbojet engine.

This phenomenon was again mentioned by Davidson and Umney in England in 1947 (Reference 2), by Ferri and Nucci in 1948 (Reference 3) and is compared to power plant surge in general by Pearce in Reference 4. Stoolman, in Reference 5, gives a brief discussion of Oswatitsch's experiments and mentions similar results which he found in tests of the same size and type model operated over the Mach number range from 1.8 to 2.5. However, since Stoolman was concerned principally with the possibility of self-excited oscillations arising from the intrinsic character of the compression system in front of an open duct with low mass flow, he did not analyze the high mass flow instability for ducts with central bodies.

In spite of the fact that the occurrence of this phenomenon has been known for more than 10 years, it has not yet been adequately explained. The investigation described herein is presented in an effort to give a clear physical understanding of this process.

1. Discussion of Steady Operation

The essential features of steady supersonic diffuser performance can be shown quite effectively by the approximation of 'one-dimensional' gasdynamics. Although the theory is simple and well known, it is reproduced in detail here for the intuitive feeling, or insight, which the derivation affords. An understanding of the different aspects of steady operation is helpful in gaining a physically clear picture of the instability.

The important features of a supersonic ramjet engine with a central body diffuser are shown in figure 1.

The free stream and exit stations are denoted by 0 and 6 respectively. The end of subsonic diffusion is at station 2 and combustion is complete at station 4. Station 5 is the sonic point after combustion. Station 1 is introduced so that subsonic and supersonic compression regions can be distinguished. It is loosely defined as the beginning of uniform subsonic flow. Station 3 is used for cases in which it is desired to isolate the burner drag force. Although not all these stations are important in a discussion of diffusers, they are used here for the sake of consistency with established practice.

The area of a local stream tube is designated as S, the local state variables of the gas by the customary symbols P, ρ, T, and the Mach number as M. Local stagnation values are denoted by the subscript s, and local sonic values by the conventional star subscript. Repeated subscripts are placed on the same line for the sake of simplicity. Thus the free stream stagnation pressure is written P_{so} rather than P_{s_o}.

1.1 Development of Steady Flow Theory

The relation between stagnation pressure ratio across the diffuser, and mass flow, is obtained directly from the condition of mass conservation. The rate of mass flow past any station is

$$m = \rho SM\sqrt{\gamma RT} = \frac{PSM}{\sqrt{T}}\sqrt{\frac{\gamma}{R}}$$

where γ and R are specific heat ratio and gas constant respectively. Mass conservation across the diffuser is therefore expressed as follows:

$$\frac{P_0 S_0 M_0}{\sqrt{T_0}} = \frac{P_2 S_2 M_2}{\sqrt{T_2}}$$

In terms of stagnation conditions, this can be written:

$$\frac{P_{s0}}{\sqrt{T_{s0}}} S_0 M_0 \frac{\sqrt{\frac{T_{s0}}{T_0}}}{\frac{P_{s0}}{P_0}} = \frac{P_{s2}}{\sqrt{T_{s2}}} S_2 M_2 \frac{\sqrt{\frac{T_{s2}}{T_2}}}{\frac{P_{s2}}{P_2}}$$

Noting that diffuser flow is essentially adiabatic, and solving for stagnation pressure ratio, one obtains:

$$\frac{P_{s2}}{P_{s0}} = \frac{S_0}{S_2} \frac{M_0}{M_2} \frac{\sqrt{\frac{T_{s0}}{T_0}}}{\sqrt{\frac{T_{s2}}{T_2}}} \frac{\frac{P_{s2}}{P_2}}{\frac{P_{s0}}{P_0}} \tag{1}$$

But since this relation could also be applied between upstream and downstream sonic points, it follows that

$$\frac{P_{s2}}{P_{s0}} = \frac{S_{*0}}{S_{*2}} \tag{2}$$

The condition expressed by equation (1) therefore can be related to equation (2) by a tautology as follows:

$$\frac{P_{s2}}{P_{s0}} = \frac{S_0}{S_2} \frac{\frac{S_{*0}}{S_0}}{\frac{S_{*2}}{S_2}} \tag{3}$$

The area ratio, S_0/S_2, is a dimensionless expression of the mass flow entering the diffuser. In practice it is convenient to refer the mass flow to the critical (or supercritical) value. Thus one writes the area ratio in terms of the critical capture area, S_{oc}, as follows:

$$\frac{S_0}{S_2} = \left(\frac{S_0}{S_{oc}}\right)\left(\frac{S_{oc}}{S_2}\right)$$

The relative mass flow is now a measure of how close the diffuser is to its critical point. The remaining factor is a design constant specified for a given engine by such requirements as fuel-air ratio, combustion velocity, etc.

The mass conservation condition for a diffuser therefore results in the following relation:

$$\frac{P_{s2}}{P_{so}} = \frac{S_o}{S_{oc}} \left(\frac{S_{oc}}{S_2}\right) \left(\frac{\frac{S_{*o}}{S_o}}{\frac{S_{*2}}{S_2}} \right) \qquad (4)$$

1.2 Significant Features of Steady Diffuser Performance

A qualitative picture of diffuser performance as a function of relative mass flow can be obtained from equation (4), and general considerations based on the shock configurations in Figure 2.

In the supercritical condition (Figure 2a), and at a constant free stream Mach number, the mass flow is constant and the stagnation pressure ratio is fixed by the plenum chamber Mach number. In this condition the stagnation pressure ratio will increase as M_2 decreases (resulting from increased heat addition or reduced exit area). The maximum value is determined by the shock configuration for which the internal shock system is as near the inlet as possible.

If still more heat is added, or the exit area is reduced further, the first shock of the internal system moves outside and intersects the cone shock; the entering mass flow is reduced by spillage in the subsonic region between the subcritical shock and the inlet. For the case shown in Figure 2b the shock system efficiency is about the same as for the critical mass flow condition. The overall diffuser efficiency increases slightly as the mass flow decreases due to reduced losses in the internal passage.

At low subcritical mass flows, the shock configuration shown in Figure 2c occurs. The distinctive feature of this case is that some of

the flow entering the diffuser passes through a single shock of the strong family. The entropy rise (or stagnation pressure loss) across this single strong shock is greater than that across the two shocks inside the intersection. The average stagnation pressure in the plenum chamber therefore decreases as the percentage of high entropy air in the inlet increases.

It can be seen on the basis of these qualitative considerations that diffuser performance for steady operation over a range of mass flows must be as shown in Figure 3.

The dashed line in Figure 3 is the relation defined by equation (4) for constant exit area (hence constant M_2).

2. Discussion of Experimental Diffuser Characteristics

No mention has been made up to this point of the effect of unsteady operation. All the features shown in Figure 3 have been explained in terms of steady diffuser flow. Although the occurrence in practice of such operation is rare, a few cases have been observed. An example is shown in Figure 4a.

It is interesting to note that the essential features of the steady operation performance curve are the same as for unsteady operation, or buzz. This is shown in Figure 4b where unstable operation commenced when the higher entropy air first entered the inlet, so that the region of reduced efficiency corresponded to the unstable range of mass flows.

As noted in Figure 4, the central bodies were slightly eccentric relative to the cowls. The fact that entrance of the high entropy air coincided with the onset of instability for one case and not for the other might be due to the difference in magnitude of this eccentricity. It also suggests that this event (i.e., entrance of high entropy flow) may, in some cases, result in instability. It is emphasized, however,

that the data in Figure 4a show this condition alone cannot be sufficient for instability. The fact that it is not necessary is shown by the data in Figure 5.

In each case the stream tube surface passing through the intersection of the subcritical shock with the central body shock was outside the cowl when instability occurred. In Figures 5a and 5c the cone surface Mach number was too low to allow branching of the strong subcritical shock near the surface; therefore no entropy discontinuities of any kind entered the inlet. These cases show that entrance of entropy discontinuities is not necessary for instability. For the diffuser shown in Figure 5b, the high entropy air following the strong subcritical shock was well outside the cowl when instability occurred.

The linear relation for sonic exit velocity at the throttle area for which high entropy air first entered is shown in Figure 4. Since the slope of the line in Figure 4b is much greater than the steady performance curve, it is apparent that instability could not be caused by static divergence of the diffuser following entrance of the high entropy air.

The buzz phenomenon is easily recognized either by optical observation or by observation of plenum chamber pressure with a system capable of following high speed transients. In wind tunnel work, the easiest way to observe it is by either schlieren or shadowgraph observation of the diffuser shock system. The characteristic features of the oscillation are shown in Figures 6 and 7.

Not only is the optical method an easy way to detect the presence of buzz, but it also yields some understanding of the phenomenon. It can be seen in Figure 6, for example, that the downstream limit of shock travel during the oscillation is the supercritical configuration.

Another important observation is that the range of shock travel does not depend much on the average mass flow. In fact, by careful adjustment of the exit throttle it is possible to set the mass flow so close to the transition point that several minutes can elapse between individual cycles without affecting the range of shock travel. The interval between oscillations is random; the performance of the diffuser during this interval is the same as in the steady subcritical range above the transition point. By observation of the schlieren screen, the period of an isolated cycle can be seen to be on the order of 0.2 seconds or less.

Viewed by itself this information, obtained simply by observation with conventional schlieren or shadowgraph methods, would be little more than suggestive; when combined with transient pressure measurements, however, a clear picture of the oscillation can be obtained.

3. Description of Model and Equipment for Transient Flow Tests

In model testing technique the similarity parameters for steady phenomena are Mach number, Reynolds number, and geometric similarity. Consideration of the effects of these parameters is sufficient for the determination of diffuser characteristics in the region of steady operation. However, when the operation is transient some characteristic time enters the picture. For problems where wave propagation is important the significant time is essentially the ratio of the overall length to the stagnation speed of sound. Where the buzz phenomenon is important, it will be seen later that the important time is effectively that required to fill the plenum chamber at a flow rate equal to the difference between the supercritical value and the exit flow rate. This means that small models, often used in diffuser research work, on the

order of 6 inches to one foot in length are not adequate for investigation of transient phenomena in full scale engines.

The model which was instrumented for pressure measurement had a plenum chamber diameter of 5.25 inches and could be adjusted in length to 96 inches, 120 inches, or 140.4 inches by inserting cylindrical spools. It was equipped with pressure transducers located at three stations on the central body, and at one station in the plenum chamber.

Scale drawings of the model, showing the three lengths tested, and transducer stations, are shown in Figure 8. It had a 20° cone central body, a critical capture area at Mach number 1.95 which was 27.7% of the plenum chamber area, and a cowl lip coordinate angle of 33.8°.

Cold flow data for this diffuser are shown in Figure 5b. It reached a critical point stagnation pressure ratio of 0.882 but had a transition point (from steady subcritical to buzz) at 99% of critical mass flow.

The engine was equipped with a conventional can-type burner operating on gasoline fuel. It was installed for combustion tests in the 120 inch length engine only. The purpose of the combustion tests was to determine the influence of buzz on cumbustion, the effect of heat addition on buzz, and transient pressure variations during burning and blowout.

A standard Wiancko system was used for the pressure measurements. This consists of a carrier oscillator driving an a.c. bridge at three thousand cps. The two active arms of the bridge consist of coils mounted in the transducer. The a.c. current resulting from an unbalance of the bridge is demodulated by a full wave crystal diode rectifier, and used to drive the recording equipment, which for these tests was a Heiland oscillograph with 450 cps elements. The flat response range of these gal-

vanometers, with damping, was only 275 cps.

Special diaphragm-type transducers were built for these tests by the Wiancko Engineering Company. The diaphragm and coils were assembled in a cylindrical tube nine sixteenths inches in diameter by one inch in length, exclusive of electrical terminals, which was threaded on the outside so that it could be screwed into place in the central body. It was designed for a maximum differential pressure of 100 psi to give a high diaphragm natural frequency (3500 cps). Acoustic resonance of the transducer was 2500 cps. Since these frequencies were so high, no damping was used. In the range of differential pressures encountered in the tests, roughly 20 psi, the transducers were linear within one percent of the restricted full scale value.

Unfortunately, however, due to the limited time allowed for development, it was not possible to avoid a rather large variation of sensitivity and zero drift with temperature. For the temperature range encountered in these tests changes in sensitivity, from room temperature to the operating temperature of the airstream, were as large as 15%. Zero drift effects were roughly one third of the sensitivity changes. Combined errors due to temperature could have been as large as 20%.

For this reason oscillograph records presented herein are presented as they were taken, without reference to a pressure scale. This is actually not a serious limitation in the interpretation of the pressure records.

An idea of the order of magnitude of the pressure variations during the oscillation can be obtained from Figures 14, 15 and 16. These figures were prepared from photographic enlargements of the oscillograph records to give the same time scale. Approximate corrections for sensitivity and zero drift were made by comparing the measured pressures to

such reference values as critical point plenum chamber pressure and the supercritical pressure at the transducer station nearest the inlet. With these corrections, the curves were then drawn by hand by careful comparison with the oscillograph records. It is believed the accumulated errors in Figures 14, 15 and 16 are not larger than 10%.

It should be mentioned before leaving this subject, that improvements have been made in the technique of transient pressure measurement since these data were taken.

Standard Wiancko bourdon tube-type transducers are used, in a temperature-controlled wind tunnel; data are recorded on a Consolidated oscillograph. Non-linearity effects, roughly 1% to 2% in the galvanometer and 0.25% to 0.5% in the transducer are compensated by calibration. Since the wind tunnel stagnation pressure can be set and controlled to a given value within 0.2%, it is possible to superimpose on the oscillograph record a grid of constant pressure lines spaced at even tenths of the stagnation pressure so that the data appear on the record in reduced form.

With reasonable care, calibration and setting of the galvanometers can be determined within $\pm$ 0.01 inches, or 0.25% of a 4 inch full scale range. Transducer errors due to temperature are less than 2% per 100° F change for both zero drift and sensitivity change. Since the model temperature with the tunnel running is not more than 25° F above room temperature, errors due to this source are not greater than 0.5%.

Therefore, if only one channel were used, and the pressure scale were set to compensate its non-linearity, the maximum total error would be 1.55% and the probable error 0.52%. If several channels

were used, with an average compensation for non-linearity, the total error would be 2.80% and the probable error 0.95%.

The wind tunnel had a test section 17 x 20 inches in size, and was operated non-return, without drying or temperature control. Air was supplied by a stand-by blast furnace compressor at the Kaiser steel mill located at Fontana, California. This wind tunnel was a part of the Fontana Aeronautical Laboratory operated by the University of Southern California Engineering Center until 1948. This facility has been relocated at NAMTC, Pt. Mugu, California. It is now known as the Aerodynamic Test Division and is still operated, under contract from Pt. Mugu, by the Engineering Center.

The nominal Mach number of the tunnel was 2.00; during the test period it averaged 1.95 with a variation of ± 0.03 due to humidity effects. The stagnation temperature of the air stream averaged 200° F with a variation of ± 25°.

4. Discussion of Experimental Results

Typical oscillograms are reproduced in Figure 9, showing the effect of average mass flow through the diffuser on pressure fluctuations at the 4 transducer stations for the intermediate volume. Referring to the figure, vertical orientation of the traces down the page corresponds to downstream orientation of the transducers in the model. Vertical timing lines occur at 0.01 second intervals.

The important features of the oscillation are clearly shown in Figure 9. At zero mass flow all stations show the presence of a high frequency, periodic oscillation at about 600 cycles per second. At 18% of critical flow the same high frequency oscillation is apparent,

but a different phenomenon has now appeared. A random oscillation with a much higher amplitude and longer period (about 0.035 seconds) now appears in addition to the high frequency motion. At 41% of critical flow the long period motion is dominant; it is more nearly periodic, although still random, and the period has increased to about 0.040 seconds for an isolated cycle. The high frequency motion is still present although it occurs in bursts at intervals which show a consistent relation to the long period cycle. Its frequency is now about 700 cycles per second. At 66% of critical flow the long period oscillation has acquired a wave form which is characteristic of this phenomenon for all higher mass flows between this value and the transition point.

It appears that the transient operation consists of a mixture of two intrinsically different phenomena. One is a high frequency, periodic oscillation which occurs without interruption only at very low flows. The other is a relatively long period motion with a fairly definite period for each cycle, depending on mass flow, but with a random time interval between cycles. Although the high frequency oscillation is present at all mass flows below the transition point, it is not actually superimposed on the long period motion. The long period motion blocks out the high frequency oscillation over part of its cycle; the interval during which it is not blocked occurs consistently at the same phase of the long period motion.

Oscillograms showing the effect of plenum chamber volume on the transient pressures just below transition are presented in Figure 10. The second trace from the inlet, for the smallest volume case, should be disregarded. The diaphragm of the transducer located at that station was broken during the run.

In addition to the transient pressure measurements, schlieren pictures of the inlet shock system were taken at a repetition rate on the order of 2 to 3 thousand frames per second. These data, shown in Figure 11, were taken for the small engine volume case only, using a Fastax camera with a rotating prism type shutter; which accounts for the poor resolution. The apparent asymmetry of the cowl is due to interference from a prism mounted in the center of the schlieren system. Although it blocks off part of the cowl, the field of view is clear up to the cowl inlet. The schlieren system was illuminated by a General Electric BH-6 mercury vapor bulb operated from a 60 cycle source. The underexposed regions therefore occur at 1/120 second intervals.

The shock motion during the high frequency pressure oscillation at zero mass flow can be seen in Figure 11a. Instead of a strong stationary shock of the type found in front of a sphere, for example, a high frequency pulsation of the strong shock is observed. Its frequency, determined by counting frames, is 607 cycles per second which agrees with the high frequency pressure oscillation at zero mass flow in Figure 9. The short burst of high frequency oscillation noted above for high mass flows can be seen in Figure 11b. The shock pulsation has the same appearance as in the zero mass flow case, but the frequency has increased to 690 cycles per second.

4.1 Organ Pipe Oscillation at Low Mass Flow

Before proceeding with an analysis of the long period cycle, it is interesting to see how much can be said about the high frequency motion.

The physical length of the small volume engine (from cowl lip to

exit) was 7.83 feet and the stagnation speed of sound was 1260 feet per second. The exit nozzle for the high mass flow case consisted of a circular hole in a 1/2 inch thick flat plate. The only contraction from the plenum chamber diameter of 5.25 inches to the exit diameter of 2.53 inches was a conical frustum, formed by a 45 degree bevel in the 1/2 inch plate with its apex downstream. The downstream end of the plenum chamber was therefore essentially a flat plate with a small circular hole in the center occupying 23.2% of the base area.

For the zero mass flow oscillation, the wave length is only 2.08 feet. Since the engine length is 7.83 feet, the theory of the Helmholtz resonator cannot be used to explain this high frequency motion. It can, however, be accounted for in terms of wave propagation. Since the diffuser central body extends only 2 feet downstream from the cowl lip, even the short engine must behave essentially like an organ pipe. At zero mass flow the exit is closed, and in the high subcritical range is only 23.2% open. The reflection in the latter case is simply an attenuated wave of the same type as for the closed end reflection. The experimental frequencies are compared below to the 8th and 9th modes of a closed-end organ pipe.

Mass Flow	Exp. Freq.	Closed End Mode	Organ Pipe Freq.
0	607	8	604
during buzz	690	9	685

TABLE I Comparison of Experimental and Theoretical Frequencies for Short Engine

The fact that the oscillation is so far from the fundamental mode suggests that the frequency must be determined roughly by the driving mechanism. The actual frequency is then fixed by the nearest resonant

mode of the pipe. The forcing function is not understood. However, a similar high frequency oscillation has been noticed at low mass flows in tests on diffusers without central bodies. In both cases the cowl leading edge has been sharp. This suggests vortex shedding from the cowl lip as the forcing function, as well as the frequency determining factor. It is not clear why the frequency should be higher when the exit is partially open, although this behavior seems to be characteristic of the oscillation.

Results similar to these have been observed on a small diffuser model tested at Mach number 2. This model was only 1.89 feet long, from the cowl lip to the exit, but its transient characteristics were qualitatively similar to those of the large engine.

Due to the small scale, the buzz (long period oscillation) had a much shorter period than that for the large engine, but the low mass flow oscillation had essentially the same frequency. At zero mass flow, the high frequency oscillation occurred at 470 cycles per second. At the test value of the stagnation speed of sound (1160 feet per second) the second mode of a closed end organ pipe 1.89 feet long is 460 cycles per second. This note was clearly audible. As the mass flow was increased (below the buzz range) the note suddenly increased pitch by a little less than an octave, and the shape of the shock region in front of the inlet changed at the same instant. The actual frequency was not measured at the time. However, the third organ pipe mode is 767 cycles per second (a ratio of 5/3) which agrees with the observed change in pitch. Results of these two tests are summarized below:

Diffuser Length (Ft.)	Mass Flow	Exp. Freq.	Mode	Freq.	R_N (Based on cowl diameter)
7.83	0	607	8	604	0.72×10^6
7.83	0	690	9	685	0.72×10^6
1.89	0	470	2	460	0.74×10^6
1.89	0	940	3	767	0.74×10^6

TABLE II Comparison of Frequencies for Diffusers of Different Length

These data indicate there must be some forcing function relatively insensitive to frequency in the range from 400 to 800 cps, with the actual frequency determined by the nearest organ pipe mode. Since both frequency and Reynolds number are essentially constant for all cases, it is suggested that vortex shedding from the sharp cowl lip might be the forcing function. It is felt that the experimental evidence justifies this as a reasonable hypothesis; verification of the vortex shedding mechanism through a separate experimental program would be necessary before it could be accepted, of course.

The main purpose of the present investigation, however, is to explain the long period buzz oscillation. Although an understanding of the high frequency oscillation would be both interesting and valuable, it is not necessary for the present problem. It is sufficient to observe its presence during the phase of the buzz cycle in which the strong shock appears in front of the inlet.

4.2 Analysis of Buzz

It can be seen in Figure 10a that the short burst of high frequency oscillation for the short engine operating at high mass flow has a duration of about 0.018 seconds. By counting frames in Figure 11 it can be seen that the strong shock is in front of the inlet for an interval of 0.0185 seconds. This shows that the high frequency burst,

seen in the oscillograms just before the inlet pressure trace drops off, corresponds to the interval during which the strong shock is in front of the inlet. Events before and after this interval, shown on both the pressure record and schlieren film, can therefore be correlated.

From the film it can be seen that the diffuser shock system becomes supercritical immediately after the high frequency oscillation stops. By counting frames, it is found that this persists for 0.036 seconds, after which steady subcritical operation occurs for an arbitrary interval. As shown in Figure 10 the supercritical interval appears as the low pressure phase of the cycle for the trace nearest the inlet. This is graphically illustrated by an interval of about 0.012 seconds during which the inlet shock is downstream of the first transducer station and the local flow is supersonic. During this interval the pressure at this point is a minimum and is constant.

The total fill-up interval, i.e., the period of low pressure at the first station (Figure 10a) is about 0.050 seconds. Apparently the inlet first becomes subcritical after 0.036 seconds, and reaches equilibrium subcritical operation 0.014 seconds later at a slightly higher pressure. The buzz cycle has now ended; steady subcritical flow is established and persists for an arbitrary time interval before another cycle takes place.

The oscillation is evidently a series of relaxation cycles occurring at random intervals between which steady, equilibrium, subcritical operation occurs.

Steady subcritical operation is interrupted in some manner, following which the inlet shock moves to the tip of the central body and the high frequency oscillation, characteristic of low mass flow operation,

sets in. While the inlet shock is oscillating, mass discharges from the plenum chamber with a corresponding drop in pressure. At the end of the high frequency oscillation, the inlet shock moves into the diffuser and air enters at the supercritical rate. Due to the low plenum chamber pressure, the exit flow rate is less than the equilibrium value. The net inflow is therefore positive and the plenum chamber pressure increases until the initial equilibrium point is reached. Operation is then steady until the diffuser flow breaks down again. It has been found that by careful adjustment of the exit throttle near the transition point, time intervals of several minutes between cycles can be observed.

With this qualitative description of the phenomenon in mind, a careful analysis of the pressure and schlieren data will now be made to determine the cause of the instability, the re-starting process, and the nature of the fill-up phase of a typical buzz cycle.

It can be seen in the oscillograms that deviation from subcritical flow starts first near the inlet. The time scale is not large enough to permit accurate determination of the transducer which shows the first change in pressure. It is clear, however, that the three stations on the central body show a pressure drop before the plenum chamber station does. The plenum chamber Mach number for this diffuser is 0.117 at the critical point. If this speed were added to the stagnation speed of sound (1260 feet per second), the time for a pressure wave to travel from the last central body station to the plenum chamber station would be found to be 0.003 seconds; which agrees well with the data.

Following this initial pressure drop, the high frequency oscillation sets in immediately. The time interval for the pressure drop cannot be determined accurately from these data; but for most cases it ap-

pears to be on the order of 0.002 seconds. This means that the inlet flow changes from the steady subcritical condition to high frequency oscillation in about 0.002 seconds. This is much less than the time required for particle flow through the engine, or for wave propagation from the inlet to the exit and back. At the plenum chamber Mach number of 0.117, an interval of 0.053 seconds would be required for a fluid particle to travel from the inlet to the exit of the shortest engine. The wave propagation time for the same engine would be 0.012 seconds.

Collapse of the inlet flow, i.e., from steady subcritical operation to the high frequency oscillation, has been completed in one third of the time required for an acoustic wave to reach the exit, and before a fluid particle has had time to enter the plenum chamber. It must be concluded from this comparison that conditions in the plenum chamber have nothing to do with the breakdown of steady flow at the inlet. That is, the breakdown is so sudden that the way in which it occurs cannot be affected by conditions in the plenum chamber.

The question now arises whether conditions in the plenum chamber, just before the breakdown of the inlet flow, could be the cause of breakdown. Although the plenum chamber plays no role in the breakdown per se, it is possible that conditions in the plenum chamber preceding breakdown may have been sufficient to cause the instability.

4.21 Diffuser Separation as a Possible Cause

Consider the diffuser in a condition of steady subcritical operation; and suppose the central body flow were to separate suddenly at some point in the subsonic diffuser. The central body wake would increase, and the core flow velocity in the annular subsonic diffuser around the

central body would also increase. As a result the pressure at the plenum chamber transducer would decrease. If this flow were to mix completely in the plenum chamber before reaching the exit nozzle, the result would be a decrease in both the local pressure and stagnation pressure and a corresponding decrease in exit mass flow rate. Mass would therefore begin to accumulate in the plenum chamber, which would result in a compression wave traveling upstream toward the inlet. The effect of this wave joining the inlet shock would be to move it upstream at the velocity required to match the increased pressure downstream of the shock. This motion might be unstable, beyond a certain amplitude, and result in collapse of the inlet flow.

If this argument were correct, one would expect to find a drop in pressure at the plenum chamber station as the expansion wave from the separation propagates downstream. Suppose, for example, that a separation occurred at the last central body transducer station for the shortest engine. The pressure would begin to drop at the plenum chamber station 0.0030 seconds later. Fluid from the separated region would reach the exit 0.046 seconds later, or 0.043 seconds after the plenum chamber pressure dropped. An upstream wave would then require roughly 0.007 seconds to reach the inlet. So one would expect to find a drop in pressure at the plenum chamber station about 0.050 seconds before the inlet pressure dropped. For the intermediate and long engines, corresponding values of this time would be 0.067 and 0.078 seconds, respectively. Examination of the oscillograms in Figures 9 and 10 shows that this argument must be completely inapplicable; the time intervals are too large by a factor of 10 to be related in any way to the breakdown process. It follows, therefore, that the instability is not caused by a transient accumulation of

mass in the plenum chamber following a loss in diffuser efficiency.

Since the time interval required for particle flow is too long, the question arises whether diffuser flow separation could interact on the inlet flow through wave propagation in time to cause instability.

In the diffuser flow separation argument it was observed that the exit flow would be reduced when the separated flow reached the exit nozzle. Actually the reduction would begin earlier than this. As mentioned above, the immediate effect of a central body flow separation is a pressure decrease in the core flow, which is propagated into the plenum chamber as an expansion. As the fluid moves downstream from the separation point, a low pressure region develops between that fluid and the separation point on the central body. That is, the separated region grows at the particle flow rate; which means that expansion waves are generated continuously and move into the plenum chamber. Consequently the exit pressure, and hence the exit flow rate, begins to drop when the first expansion wave from the separation reaches the exit, and drops continuously for some time thereafter.

It might be argued that mass accumulation in the plenum chamber would begin when the first expansion wave from the separation reached the exit. In the order of increasing engine length, the time intervals required for acoustic waves to travel downstream from the plenum chamber transducer to the exit and back to the inlet are 0.0088, 0.0120 and 0.0153 seconds respectively.

If this phenomenon were responsible for breakdown of the inlet flow, one would expect to find a smooth drooping of the plenum chamber pressure traces beginning at these time intervals before the sharp drop in the central body traces takes place. Furthermore, the change in plenum

chamber pressure should continue until the sharp pressure drop resulting from collapse of the inlet flow has had time to be felt at the plenum chamber station. In the order of increasing engine length these additional time intervals are 0.0038, 0.0038 and 0.0049 seconds respectively.

If the separation argument in this form were correct, one would expect to find the following situation: The plenum chamber pressure trace should begin to drop at a time interval, Δt_1, before the sharp drop representing collapse of the inlet flow, and should continue to change for an additional time interval Δt_2 before the sharp drop from the inlet has reached the plenum chamber station. In the order of increasing engine length, these time intervals are:

Length inlet to exit (inches)	Δt_1	Δt_2	$\Delta t_1 + \Delta t_2$
94	.0088	.0038	.0126
118	.0120	.0038	.0158
138.4	.0153	.0049	.0202

Examination of the pressure data in Figures 9 and 10 shows these time intervals to be too large by about a factor of two. Furthermore it should be noted that the shape of the plenum chamber pressure trace is not quite right. Since it is argued that collapse of the inlet flow is due to upstream propagation of a pressure wave resulting from mass accumulation in the plenum chamber, one should expect to find some evidence of a pressure rise following the initial drop in the plenum chamber transducer trace. Examination of the data shows this does not occur.

4.22 Instability Caused by Blocked Inlet Flow

Another approach to the instability problem can be made on the basis of a consideration of inlet flow conditions alone. In this argu-

ment the plenum chamber is not a factor in causing instability, it simply reflects the history of the breakdown within the inlet as the complete picture, from beginning to end, is propagated through the plenum chamber.

Flow in the inlet of a diffuser is far from the idealized concept of a normal shock followed by uniform subsonic flow. In reality it is similar to the shock system in a wind tunnel diffuser, in which transition to subsonic flow is accomplished through several shocks. The first shock of the train has the characteristic "lambda" form of a strong shock-boundary layer interaction. Near the surface, the flow is separated by an oblique shock of the weak family, which forms a Mach reflection with a strong shock covering the remainder of the entering flow.

The Mach number of the flow approaching the branch point is roughly 1.59; and since the downstream flow is subsonic the intersection will presumably be defined by the condition of maximum downstream pressure. The maximum pressure ratio across the lambda shock occurs when the strong shock is normal to the flow. The geometry of this shock for Mach number 1.59 is shown by the solid lines in Figure 12 for a flow direction of 10 degrees upstream from the intersection point. The deflection of 2 degrees across the oblique shocks is shown as a separation of the cone surface flow which creates a dead water region at the minimum area of the inlet and reduces the effective area available for the entering flow.

A random pressure pulse arriving at this lambda shock from downstream would increase the downstream pressure above the equilibrium value for the shock. Since the strong shock ascending from the Mach reflection is normal, it would have to assume an upstream velocity to match the increase in pressure. Calculation of the shock intersection problem for the moving shock shows a corresponding increase in deflection angle

across the oblique shocks. An increase of 10% in pressure ratio across the normal shock would result in an upstream shock velocity 15% of the local sonic speed, and an increase in surface flow separation angle from 2 degrees to 5 degrees. The moving shock is shown by the dashed lines in Figure 12.

As long as the streamline approaching the cowl lip passes through the normal shock, the entering mass flow is essentially unaltered. However, as a result of both the forward motion and the increased separation angle, the effective inlet area available for that mass flow decreases as the shock moves forward.

If a random pressure pulse from downstream has sufficient strength to move the lambda shock far enough forward to block the inlet, mass will accumulate in the inlet and the subsequent pressure rise will force the shock to diverge to the cone tip. As the forward velocity of the shock increases, the separation angle increases also. At some point the deflected flow by-passes the entrance entirely and the entering flow is cut off. Spark pictures of the shock during divergence have shown surface flow deflection angles as large as 17 degrees.

As a result of the abrupt interruption of the flow, the moving air column within the diffuser creates a sharp pressure drop at the inlet, which then propagates downstream through the engine.

The divergent motion of the shock, and the subsequent high frequency oscillation of the shock near the cone tip, can be seen in Figure 11b.

The time for divergence of the shock in Figure 11b is 0.0022 seconds; which agrees well with the interval of 0.002 seconds required for the abrupt drop in inlet pressure in Figures 9 and 10.

This argument would explain why the buzz cycles occur more frequently as the mass flow is reduced. Since the average position of the inlet shock moves forward with decreasing mass flow, a weaker pulse is capable of blocking the inlet. Thus a shorter interval of steady operation is possible, on the average, before such a pulse occurs.

The question now arises as to why the plenum chamber pressure droops about 0.005 seconds before the inlet pressure begins to drop. An acoustic wave requires 0.0038 seconds to travel from the inlet to the plenum chamber station (for the two shorter engines). This means that if the plenum chamber pressure droop were caused by something in the inlet, it would have started 0.0088 seconds before the sharp pressure drop at the inlet occurred. It appears, therefore, that the inlet blocks about 0.0088 seconds before the entering flow is deflected sufficiently by the advancing shock to by-pass the entrance.

To recapitulate, the instability develops as follows: First, the inlet shock is pushed upstream by a random pressure pulse from downstream until the inlet blocks. Some of the mass which enters the cowl begins to accumulate upstream of the point of blockage. The pressure in that region rises and results in a forward motion of the subcritical shock. This motion is unstable and continues until the flow by-passes the cowl lip. After the entering flow has been cut off, the momentum of the air column in the diffuser sustains its downstream motion for a while and results in a low pressure region at the inlet. At the same time the mass flow entering the diffuser begins to decrease as soon as the inlet blocks, and continually decreases as the blocking progresses. The pressure downstream of the blockage point therefore begins to drop as soon as the inlet blocks. It appears from the pressure and high speed schlieren data that

the entering flow is cut off about 0.009 seconds after the inlet blocks, and about 0.002 seconds later the shock has advanced to the cone tip and the high frequency oscillation has set in.

If blockage of the inlet occurred downstream of any of the central body transducers, one would expect to see a pressure rise at that point coincident with a drop in pressure at the nearest downstream station. A good illustration of this can be seen in Figure 9h. The three downstream transducers begin to show a decrease in pressure at the last timing line before the sharp drop occurs; but the first transducer shows a rising pressure in this same time interval.

Of the three arguments given above, the last seems the most plausible, and is in agreement with the high speed schlieren and pressure data. It is believed that this explanation is correct.

Apart from acting as the source of random disturbances, the subsonic diffuser and plenum chamber have nothing to do with the occurrence of instability. The breakdown is a local condition in the immediate entrace of the inlet.

4.23 Mechanism of Re-Starting Supercritical Flow

The initial pressure drop, and subsequent high frequency oscillation have now been identified. Both the schlieren and pressure records show an average duration of about 0.02 seconds for the high frequency oscillation, or about 14 cycles at 700 cycles per second. During this time the entering flow is cut off, and mass discharges from the plenum chamber through both the exit and the inlet.

Referring again to the pressure traces in Figures 9 and 10, the next significant event is a large drop in inlet pressure caused by re-

starting of supercritical flow. Since the plenum chamber pressure is low when this occurs, the inlet flow is supersonic past the first central body station and remains supersonic for about 0.012 seconds. As mass accumulates in the plenum chamber, the pressure rises and the shock moves upstream toward the inlet. The traces at all stations show steadily rising pressure during this fill-up phase of the buzz cycle. The pressure increase in the plenum chamber is essentially due to the increase of stored mass as the diffuser approaches equilibrium mass flow. The pressure at the first station is the local static pressure at that point within the shock region, and therefore increases as the shock moves upstream.

It is interesting to note how well the downstream stations reflect the history of the breakdown at the inlet, from the initial pressure drop when the inlet blocks through the high frequency oscillation.

The immediate effect on plenum chamber pressure of the inlet re-starting appears to be a sharp rise in pressure. It can be seen in the pressure records (particularly in Figures 9f, 9g and 10b) that this is recorded at approximately the same time the abrupt drop in inlet pressure occurs, which seems to imply that the plenum chamber responds to re-starting of the inlet instantly instead of at the acoustic wave interval of 0.0038 seconds. The reason for this apparent inconsistency is shown partly by the pressure trace at the last central body station, and partly by the high speed schlieren data in Figure 11b.

The traces at both the last central body station and the plenum chamber station show the same pressure jump as the inlet re-starts, and the events are separated by the proper acoustic interval of 0.003 seconds. Since the inlet pressure drop, as supersonic flow starts over the first

central body transducer, coincides with the plenum chamber pressure jump, this means that the inlet must make an impulsive effort to re-start about 0.0038 seconds before it becomes completely supercritical.

It can be seen in Figure 11b that this is correct. The high frequency oscillation of the inlet shock continues until supercritical flow has started. Transition from the oscillation to supercritical operation occurs during the last three cycles of the oscillation, which is 0.00435 seconds at 690 cycles per second. The first motion of the shock toward the inlet occurs at the downstream limit of the excursion, and entrance of the shock occurs at the same phase of the oscillation three cycles later.

The jump in plenum chamber pressure corresponds to the first impulsive entrance of mass into the inlet, and the inlet pressure drops when supercritical flow is established three cycles later. Air in the inlet acts like a pump which delivers three impulsive surges to the internal air column to get it moving fast enough to allow the inlet to become supercritical.

4.24 Calculation of Supercritical Plenum Chamber Fill-Up

After the inlet has become supercritical, a simple approximate calculation of fill-up time can be made, based on engine volume and the known rates of flow in the inlet and out the exit. In addition to the usual assumption of one-dimensional gasdynamics, the plenum chamber pressure is assumed uniform and equal to the value given by the thermal equation of state for the mass of air in the engine, assumed to be at rest filling the entire engine volume, and at the upstream stagnation temperature.

Mass flow, m, through a sonic area, S^*, can be expressed in terms

of stagnation pressure and temperature as follows:

$$m = \left[\left(\frac{\gamma+1}{2}\right)^{\frac{\gamma+1}{2(\gamma-1)}}\sqrt{\frac{\gamma}{R}}\right] S_* \frac{P_s}{\sqrt{T_s}} \tag{5}$$

The time rate of mass accumulation within the engine is the difference between the inlet and exit flow rates.

$$\begin{aligned}\frac{dm}{dt} &= \left(\frac{\gamma+1}{2}\right)^{\frac{\gamma+1}{2(\gamma-1)}}\sqrt{\frac{\gamma}{R}}\ \frac{1}{\sqrt{T_{so}}}\left[S_{*o}P_{so} - S_{*2}P_{s2}\right] \\ &= V\frac{d\rho_{s2}}{dt}\end{aligned} \tag{6}$$

where V is the total internal volume of the engine. By use of the thermal equation of state, the density derivative can be written as follows:

$$\frac{d\rho_{s2}}{dt} = \frac{1}{RT_{so}}\frac{dP_{s2}}{dt} \tag{7}$$

On substitution of equation (7) in equation (6), one obtains:

$$\frac{dP_{s2}}{dt} = \left(\frac{\gamma+1}{2}\right)^{\frac{\gamma+1}{2(\gamma-1)}}\frac{\sqrt{\gamma RT_{so}}}{V}\left[S_{*o}P_{so} - S_{*2}P_{s2}\right] \tag{8}$$

If an effective length, ℓ, is defined such that

$$V \equiv S_2\ell$$

equation (8) can be written as

$$\frac{d\left(\frac{P_{s2}}{P_{so}}\right)}{dt} = \left(\frac{\gamma+1}{2}\right)^{\frac{\gamma+1}{2(\gamma-1)}}\frac{a_{so}}{\ell}\left[\left(\frac{S_*}{S}\right)_o\frac{S_o}{S_2} - \left(\frac{S_*}{S}\right)_e\frac{S_e}{S_2}\frac{P_{s2}}{P_{so}}\right] \tag{9}$$

where subscript, e, refers to the model exit.

By introducing $\gamma = 1.400$ and rearranging equation (9), one obtains:

$$\frac{d\left(\frac{P_{s2}}{P_{so}}\right)}{dt} + (1.2)^3\frac{a_{so}}{\ell}\left(\frac{S_*}{S}\right)_e\frac{S_e}{S_2}\ \frac{P_{s2}}{P_{so}} = (1.2)^3\frac{a_{so}}{\ell}\left(\frac{S_*}{S}\right)_o\frac{S_o}{S_2} \tag{10}$$

Equation (10) has a simple exponential solution if the exit Mach number is constant. However, since the plenum chamber pressure is low at the

beginning of fill-up, the exit Mach number may be subsonic during the initial part of the fill-up period. In the present case the engine extended so far into the wind tunnel diffuser that its exit Mach number was always subsonic, and equation (10) was integrated numerically.

Results are shown in Figure 13 for the three effective lengths tested, viz., 6.93 feet, 8.93 feet and 10.63 feet. Pressure traces for these cases are shown in Figure 10.

The fill-up curves for the 6.93 and 8.93 cases, shown as solid lines in Figure 13, demonstrate the effect of increased plenum chamber volume quite well. It is not as clearly shown for the 10.63 foot case because of the difference in plenum chamber pressure at the start of fill-up.

These results are compared to the experimental fill-up curves in Figures 14, 15 and 16. Since the condition of shock entry coincided closely with the initial rise in plenum chamber pressure, this event was used as the beginning of fill-up for all three cases.

The close agreement between the calculated and experimental curves, together with the schlieren data in Figure 11b showing supercritical flow during the fill-up period, leave little doubt that this is the correct explanation of the plenum chamber pressure rise.

The description of the buzz phenomenon is now complete. Steady subcritical operation is interrupted by choking of the inlet, which causes the subcritical shock to move forward to the cone tip and thus deflect the approaching flow outside the cowl lip. As the stored mass discharges out both ends of the engine, the engine resonates at the 9th mode for a closed-end organ pipe of the same length as the engine. As the discharge out the inlet decreases, the oscillating shock moves toward the inlet

and, after three cycles, is completely swallowed and supercritical flow is established. The inlet flow rate is then greater than the exit discharge rate and the plenum chamber fills up in an approximately exponential manner until the shock moves out of the inlet and returns to the initial equilibrium subcritical operation condition.

This explanation of the buzz phenomenon is applicable for diffusers with fill-up periods long in comparison with the period of either the Helmholtz oscillation, or the fundamental closed-end organ pipe oscillation, whichever is greater. If the fill-up period is near the period of either of these modes, the relaxation form of the buzz cycle will be distorted by dynamic effects; and if it is less than either of these periods, the corresponding mode will appear in place of the relaxation cycle even though the downstream limit of the shock travel is still supercritical. The phenomenon is then similar to buzz with respect to the forcing mechanism, but the period is determined by the mode (Helmholtz or organ pipe) rather than by fill-up time. Oscillations of this type are common in small diffuser models, of the order of a foot in length.

4.3 Effect of Combustion

With the explanation of the buzz phenomenon established it is interesting to see what effect burning has on the buzz, and also what effect the buzz has on burning.

The engine used gasoline fuel and employed a conventional can-type burner. Ignition was accomplished with a spark plug and hydrogen pilot jet. The pilot jet and spark were shut off after ignition of the main burner. The data presented therefore describe the operation of the gasoline burner alone, and are not influenced by re-ignition from the pilot jet.

A comparison of burner roughness at various fuel-air ratios is presented in Figure 17. Since these tests were made with a fixed exit area, the effect of increasing fuel flow was to move the internal shocks nearer the inlet and decrease the degree of supercritical operation. It is possible, therefore, that some of the observed increase in roughness may have been due to changing conditions within the diffuser as well as to increasing burner roughness. If the effect of fuel-air ratio alone were desired, it would be necessary to control the exit area with changing fuel-air ratio so as to hold constant diffuser conditions.

A comparison of cold flow and hot flow buzz is shown in Figure 18. It is apparent that heat addition does not alter the essential features of the buzz cycle. On the other hand, it is obvious that buzz affects burning, since the airflow through the burner varies from nearly zero to the supercritical rate during the cycle.

In most cases it was found that the extreme variations in plenum chamber conditions resulting from buzz were too severe to allow the burner to continue operating. The only way buzz during burning could be obtained was by increasing the fuel-air ratio slowly after steady burning was established. In most cases the burner would blow out immediately when buzz started. Roughly twenty tries were made before a single burning buzz was obtained.

Figure 19 shows a case of blow-out caused by the first part of a buzz cycle. The droop following blocking of the inlet, the sharp pressure drop which occurs when the inlet is by-passed, the high frequency oscillation, and the entrance of the supercritical shock can all be identified. In fact, it is interesting to note how well this record shows the presence of blocking between the first and second transducer stations. The first

central body trace rises for about 0.01 seconds before the inlet is by-passed, and the other two central body traces droop during the same interval. The plenum chamber droop starts about 0.005 seconds later and has the same duration as the central body traces.

The blowout shown in Figure 20 was due to rough burning at supercritical mass flow. The pressure fluctuations at the transducer nearest the inlet are due to the shock motion resulting from pressure pulsations in the plenum chamber. The blow-out appears to occur in two explosions; the second is much more violent than the first. The upstream propagation of the explosion waves is clearly evident in the pressure traces. The second explosion was strong enough to blow the supercritical shock out of the diffuser, following which the high frequency oscillation occurred for about 0.004 seconds.

Similar cases of blowout due to buzz and to rough burning are shown in Figures 21 and 22 where buzz occurred during burning. In Figure 21, the burner simply quit during the high frequency oscillation. When supercritical flow was re-established the flame was out and steady supercritical cold flow ensued.

In Figure 22 rough burning appears to occur just after fill-up. Apparently the heat release drops off, increases, decreases, and then increases in the form of an explosion. This entire pattern has a definite upstream propagation and clearly originates in the plenum chamber.

5. RECOMMENDATIONS

1. It is recommended that research on large scale engines with supersonic inlets be conducted to study carefully the interaction between ramjet engine roughness and diffuser instability, and between the transient characteristics of supersonic inlets and turbo-jet compressors.

2. There is need for further experimental study of the low mass flow, high frequency oscillation. An effort should be made to establish the wave character of the resonance, possibly by measurement of the nodal points along the engine axis. Also, an exploration of the pulsing flow just downstream of the cowl lip should be made, by hot wire methods, as a first step in understanding the forcing function.

6. CONCLUSIONS

1. Analysis of transient pressure variations measured in the plenum chamber and diffuser, together with high speed motion pictures of the shock movement in front of the inlet, shows the subcritical buzz (at mass flows near the transition point) to consist of a random sequence of discreet relaxation cycles. Flow entering the inlet is deflected, by the interaction of the subcritical shock with the central body boundary layer, sufficiently to block the inlet. The plenum chamber then discharges its high pressure air until the inlet can restart and fill the chamber back up to the initial equilibrium pressure.

2. At mass flows very near the transition point, arbitrary intervals of several minutes can occur between individual buzz cycles. As the mass flow is decreased the subcritical shock moves forward on the central body increasing the amount of inlet area blanketed by the separated flow from the interaction region. Hence the intensity of random pressure pulses from the plenum chamber required to block the inlet decreases, and the stable intervals between buzz cycles decreases.

3. Combustion tests showed that in almost every case tested occurrence of buzz was sufficient to result in blow out. In roughly one out of 20 attempts, it was possible to get the engine to operate in the presence of buzz for periods of 10 to 20 seconds. Examination of the corresponding pressure records showed combustion to have no qualitative effect on the buzz phenomenon.

4. At low mass flows, the instability changed abruptly from the long period buzz cycle to a high frequency oscillation. Comparison of the measured frequency with modes of a closed-end organ pipe showed good agreement with the 8th mode. When the shock was expelled during a buzz cycle a similar oscillation occurred but the frequency corresponded to the 9th mode. It is suggested that the forcing function might be vortex shedding from the sharp cowl lip at a frequency roughly determined by Reynolds number but precisely determined by the nearest resonant mode of the diffuser air column.

REFERENCES

1. Oswatitsch K., "Pressure Recovery for Missiles with Reaction Propulsion at High Supersonic Speeds (The Efficiency of Shock Diffusers), NACA TM No. 1140, June 1947

2. Davidson I. M., and Umney L. E., "Concerning the Annular Air Intake in Supersonic Flight", ARC R. and M. No. 2651, August 1947

3. Ferri Antonio, and Nucci Louis M., "Theoretical and Experimental Analysis of Low-Drag Supersonic Inlets Having a Circular Cross Section and a Central Body at Mach Numbers of 3.30, 2.75, and 2.45", NACA RM No. L8H13, November 10, 1948

4. Pearce R. B., "Causes and Control of Power Plant Surge", Aviation Week, January 16, 1950

5. Stoolman Leo, "Investigation of an Instability Phenomena Occurring in Supersonic Diffusers", PhD Thesis CIT, 1953

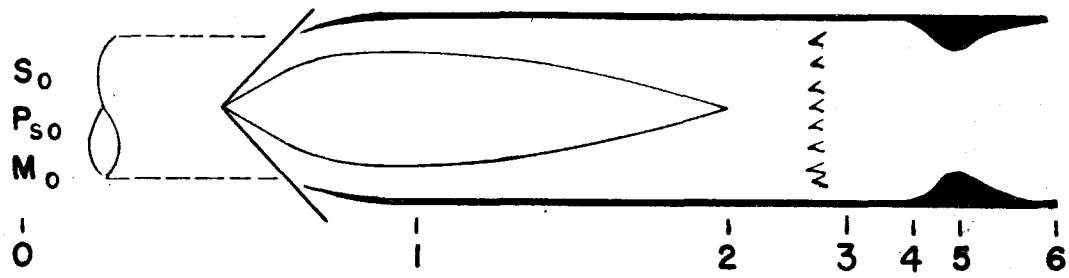

FIG. 1 STATIONS IN A RAMJET

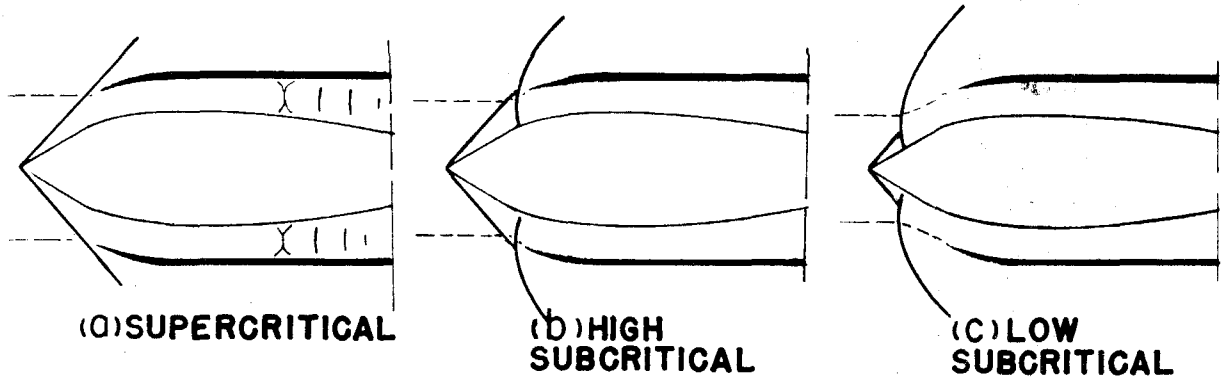

FIG. 2 SHOCK CONFIGURATIONS UNDER DIFFERENT STEADY FLOW CONDITIONS.

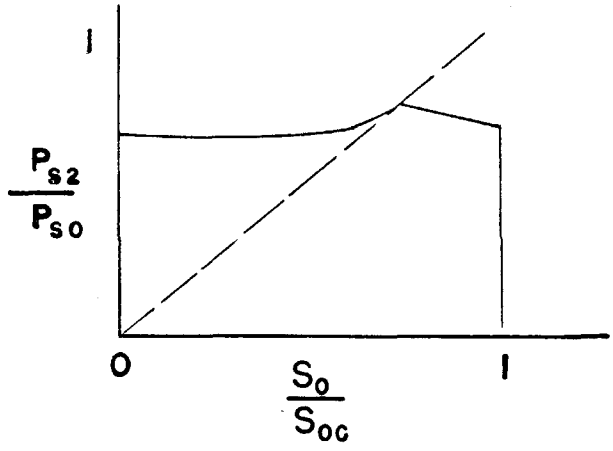

FIG. 3 TYPICAL DIFFUSER PERFORMANCE (STEADY OPERATION)

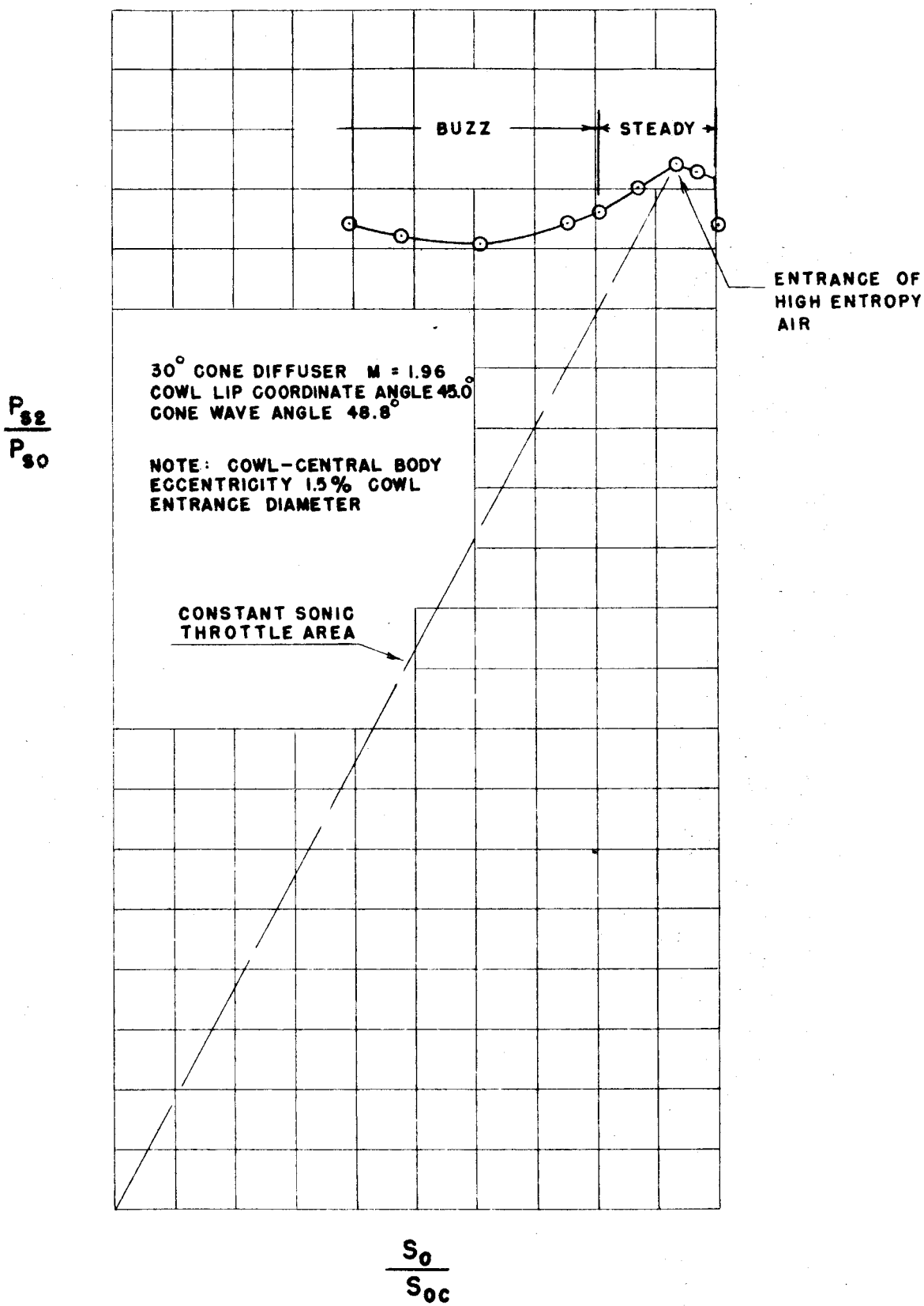

FIG. 4(a) STEADY OPERATION WITH MIXED INLET FLOW

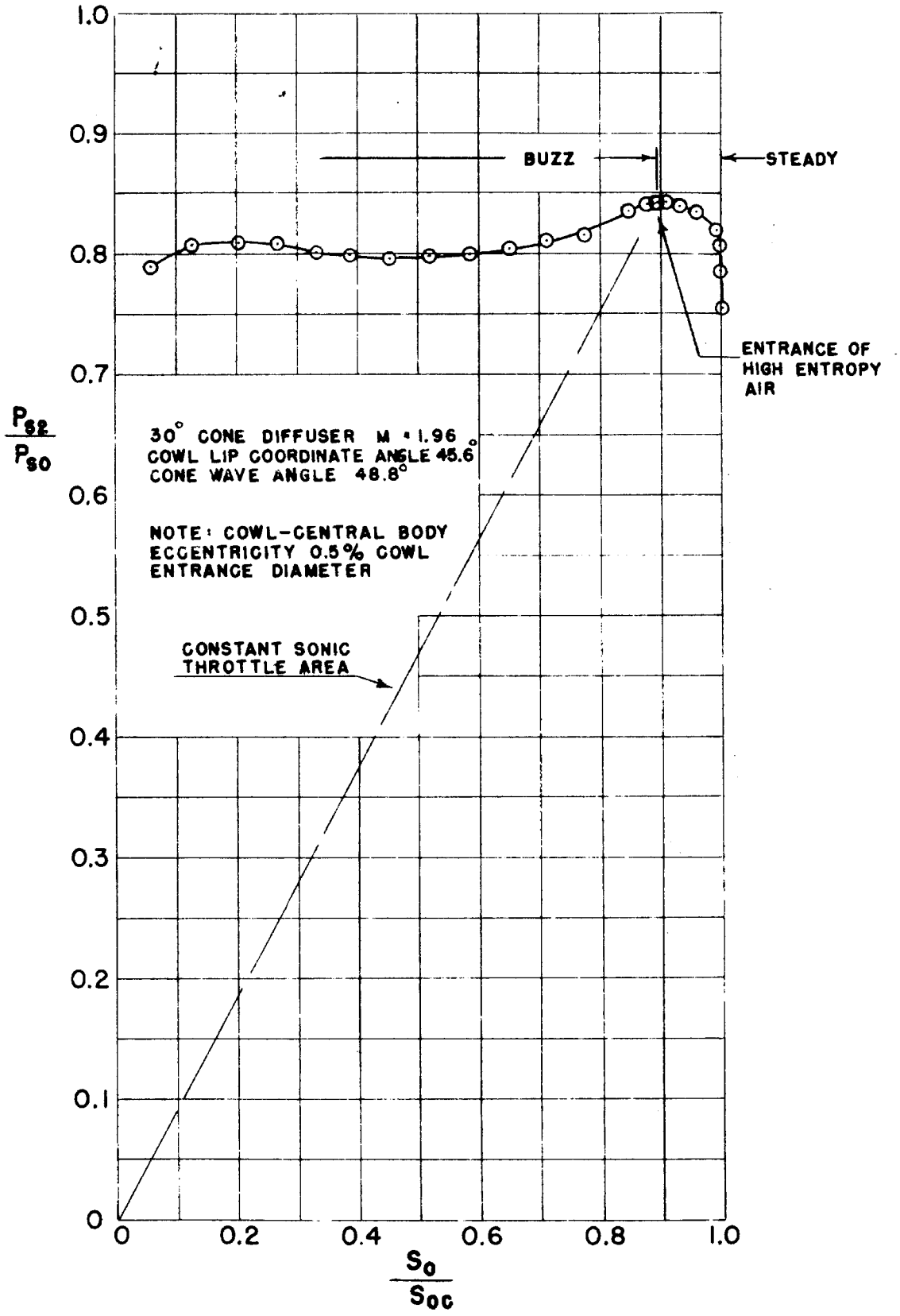

FIG. 4(b) UNSTEADY OPERATION COINCIDENT WITH MIXED FLOW

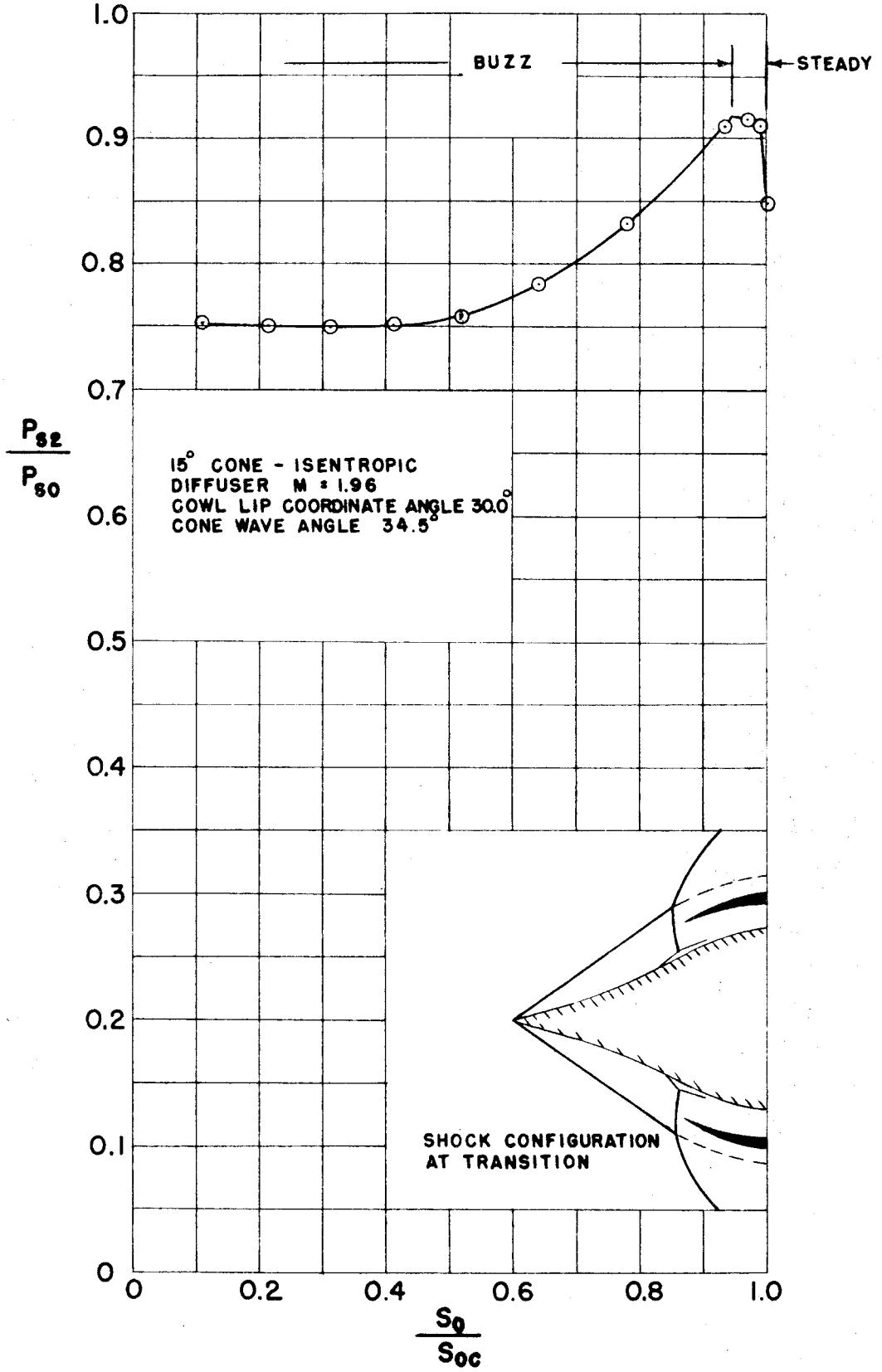

FIG. 5(a) ISENTROPIC CENTRAL BODY DIFFUSER PERFORMANCE

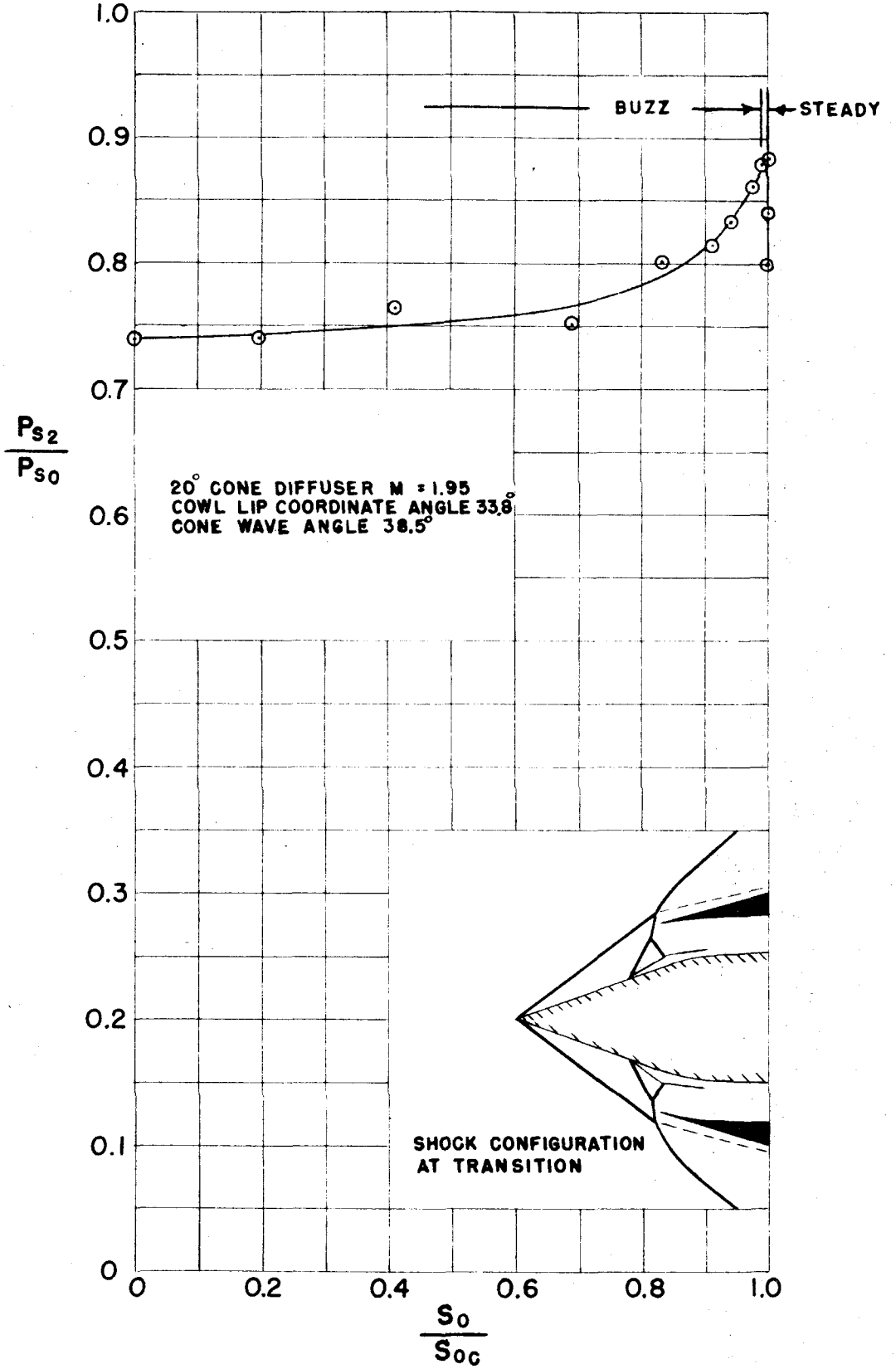

FIG. 5(b) 20° CONE CENTRAL BODY DIFFUSER PERFORMANCE

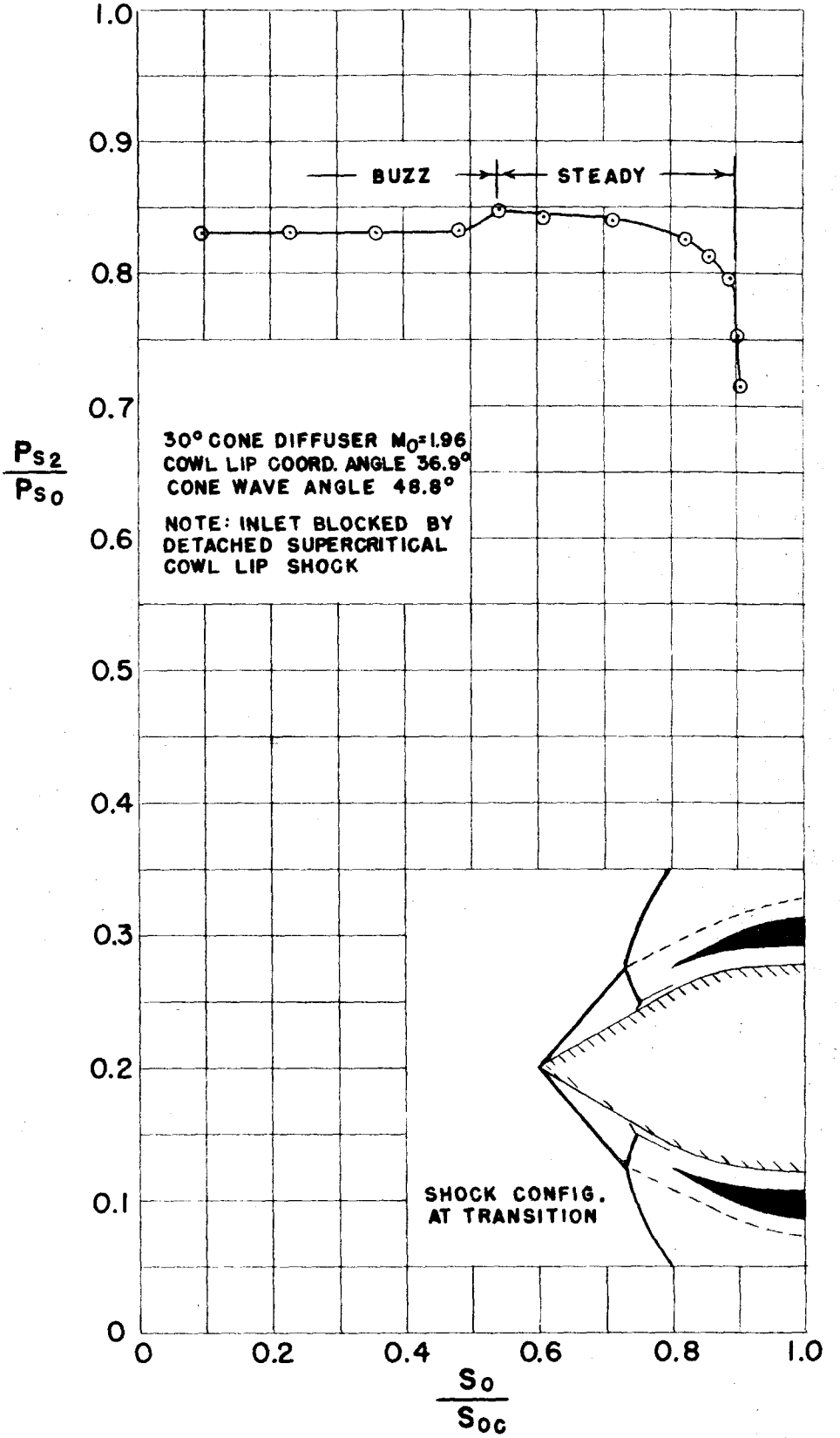

FIG. 5(C) 30° CONE CENTRAL BODY DIFFUSER PERFORMANCE

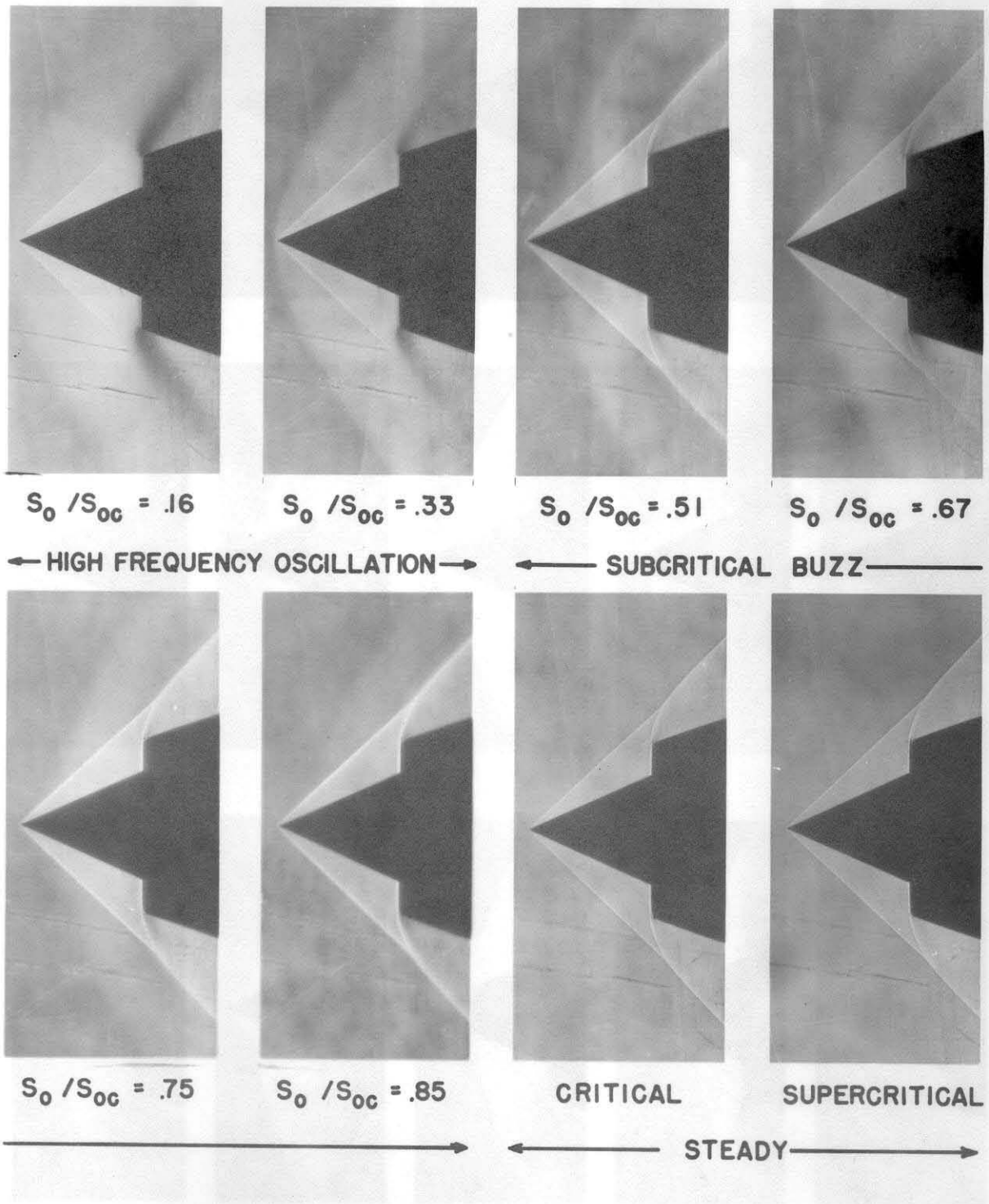

FIG. 6 EFFECT OF MASS FLOW ON INLET SHOCK SYSTEM
(25° CONE, M_o = 1.91)

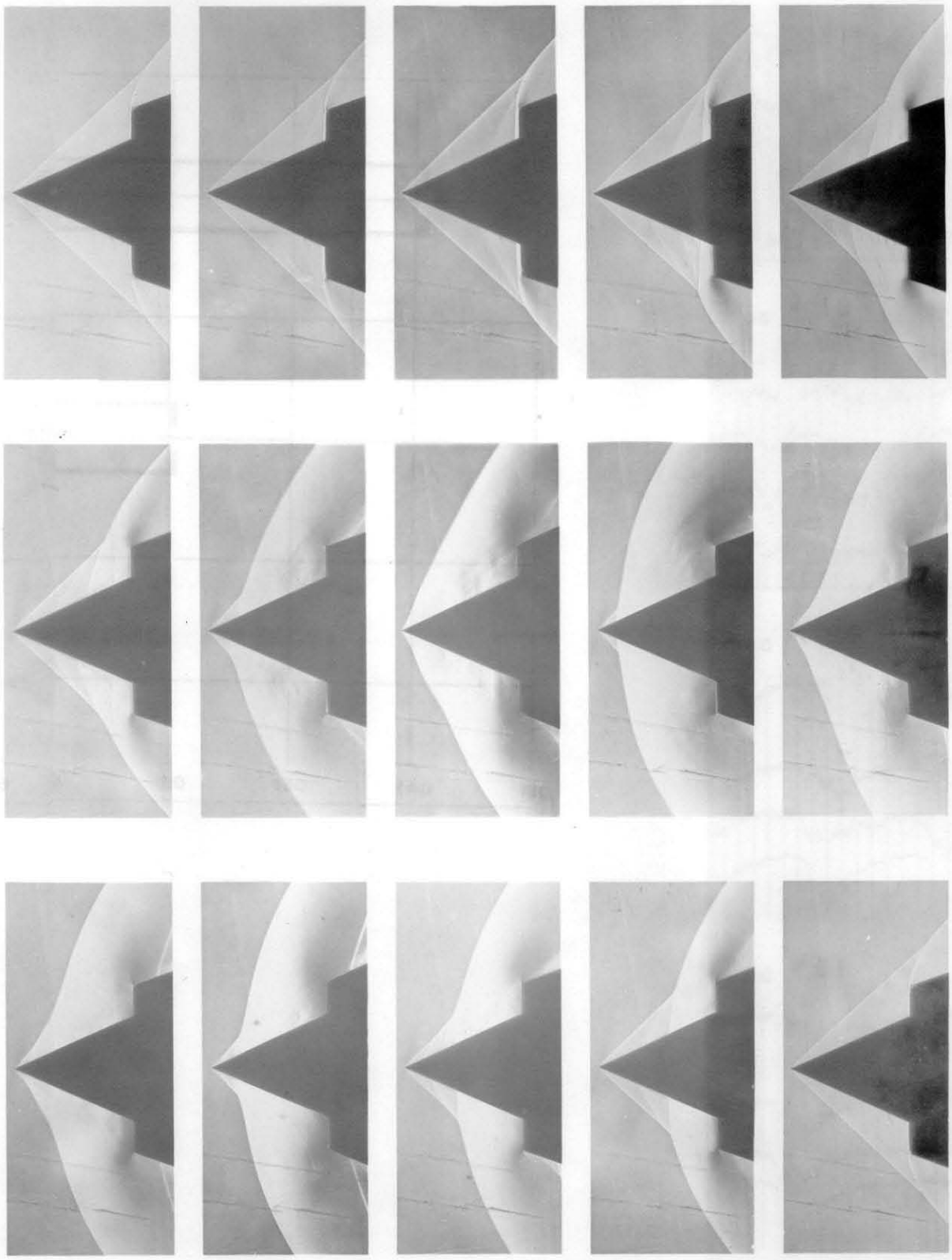

FIG. 7 SHOCK CONFIGURATION DURING BUZZ
(25° CONE, M_0 = 1.91, 4 MICRO-SECOND EXP.)

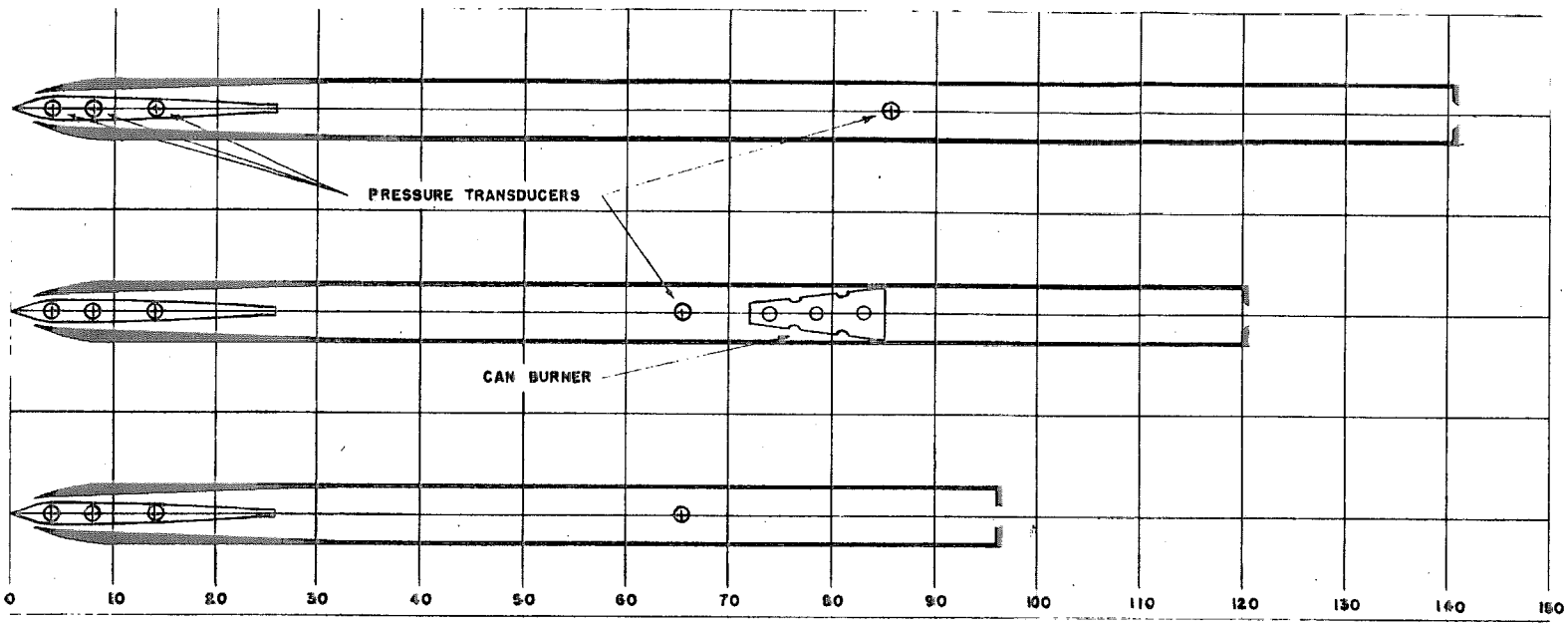

CENTRAL BODY COORD.			
X	Y	X	Y
2.664	0.968	7	1.120
2.736	0.992	8	1.100
2.808	1.016	9	1.075
2.880	1.035	10	1.040
3.024	1.067	12	0.965
3.312	1.107	14	.900
3.600	1.131	16	.835
3.890	1.145	18	.765
4.176	1.151	20	.650
4.320	1.152	22	.540
4.464	1.152	24.06	.437
6.000	1.160	26	.437

COWL COORD.			
INNER		OUTER	
X	Y	X	Y
2.154	1.440	2.154	1.440
2.304	1.468	5.675	2.510
2.592	1.520	7.000	2.750
2.680	1.566	8.000	2.885
3.168	1.606	8.500	2.925
3.600	1.650	10.812	3.000
4.032	1.680		
4.464	1.701		
2° SLOPE TO 2.625			

FIG. 8 MODEL CONFIGURATIONS

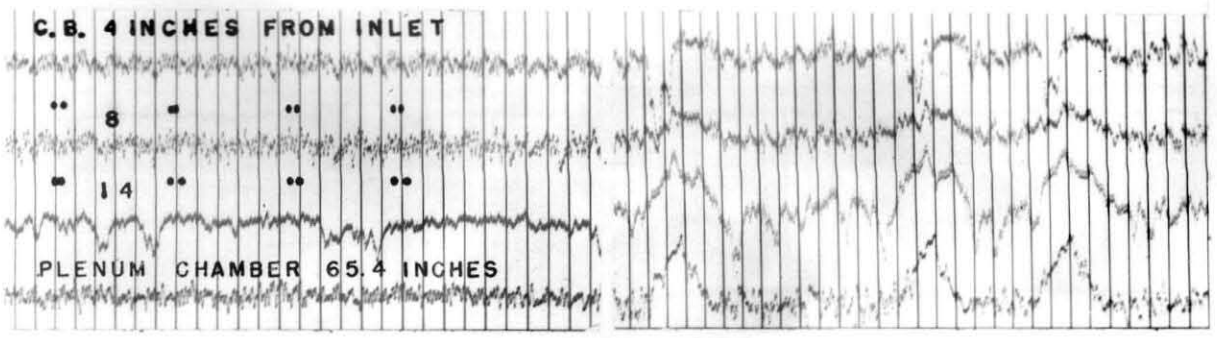

(a) $S_o / S_{oc} = 0$ (b) $S_o / S_{oc} = .18$

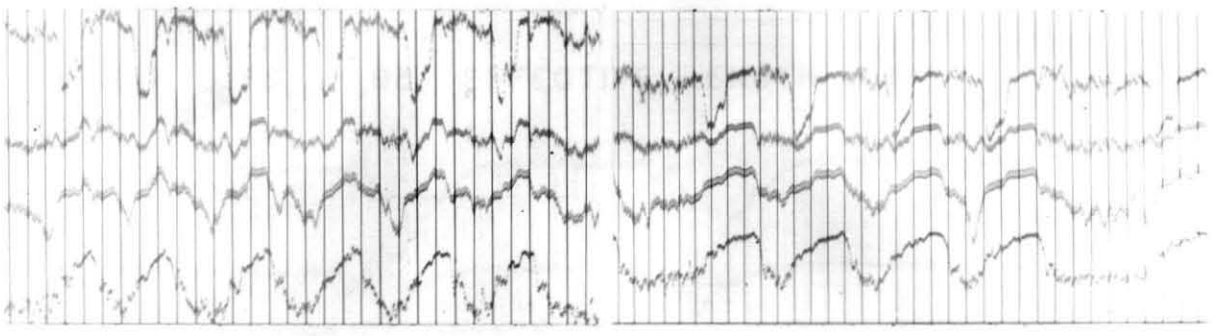

(c) $S_o / S_{oc} = .41$ (d) $S_o / S_{oc} = .66$

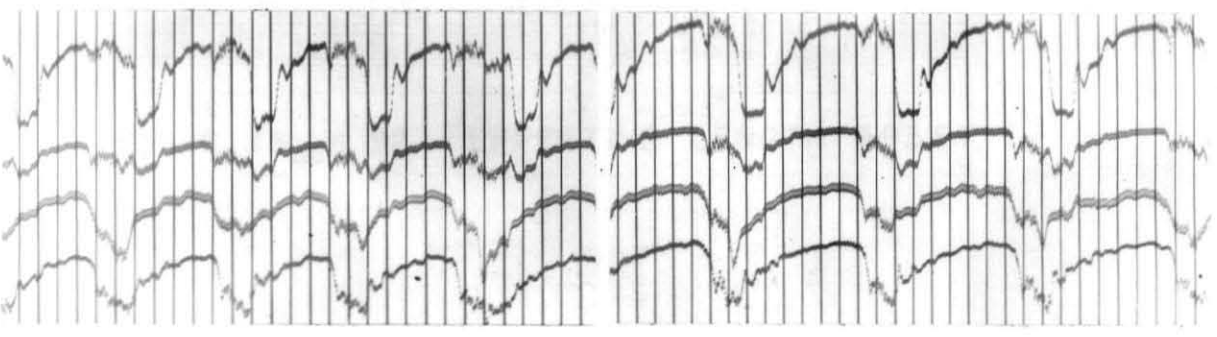

(e) $S_o / S_{oc} = .83$ (f) $S_o / S_{oc} = .91$

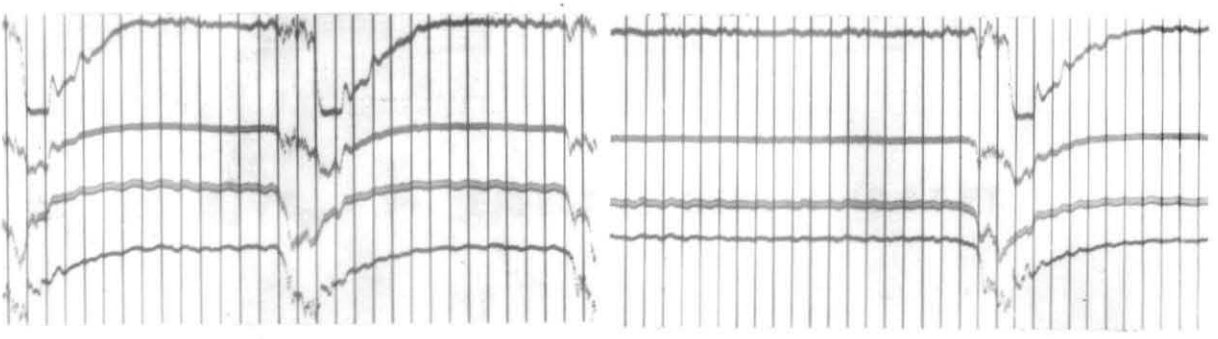

(g) $S_o / S_{oc} = .94$ (h) $S_o / S_{oc} = .98$

FIG. 9 EFFECT OF MASS FLOW ON BUZZ (EFFECTIVE LENGTH 8.93 FT.)

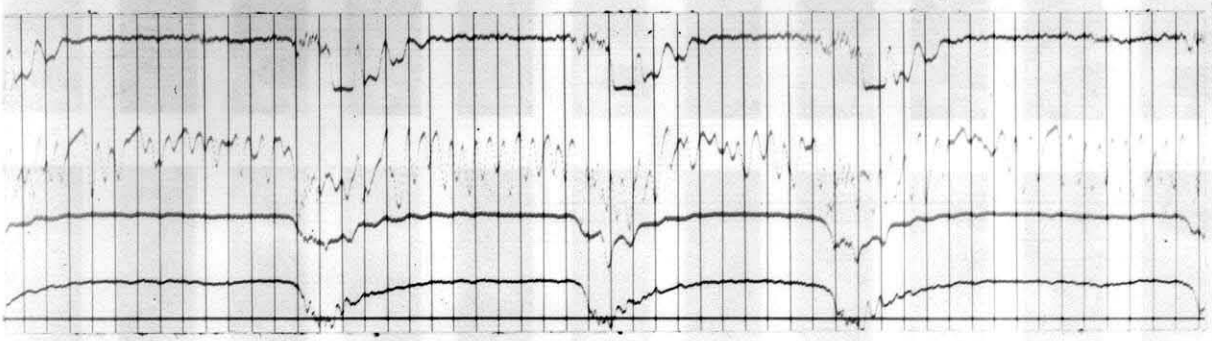

(a) $S_0 / S_{oc} = .95$ EFFECTIVE LENGTH 6.93 FT.

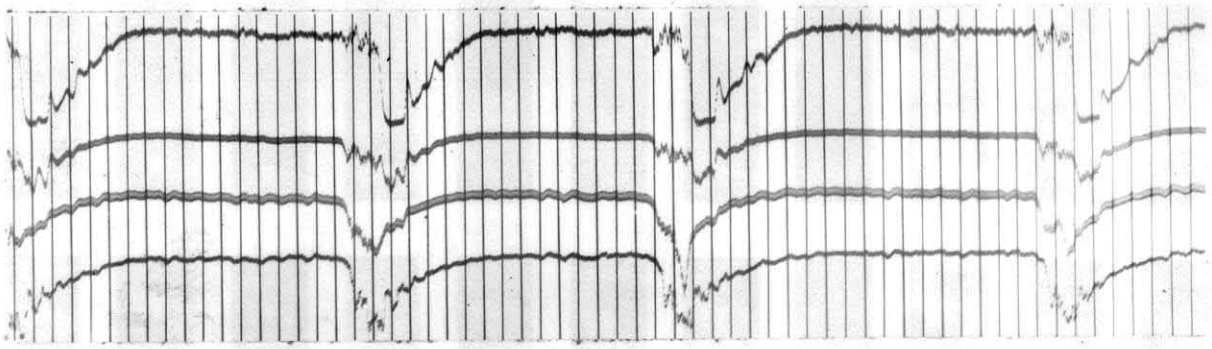

(b) $S_0 / S_{oc} = .92$ EFFECTIVE LENGTH 8.93 FT.

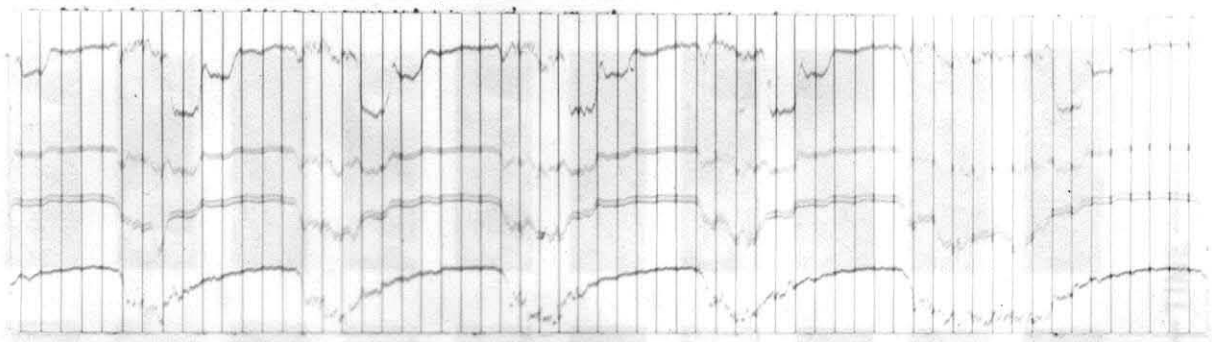

(c) $S_0 / S_{oc} = .94$ EFFECTIVE LENGTH 10.63 FT.

FIG. 10 EFFECT OF PLENUM CHAMBER VOLUME ON BUZZ CYCLE

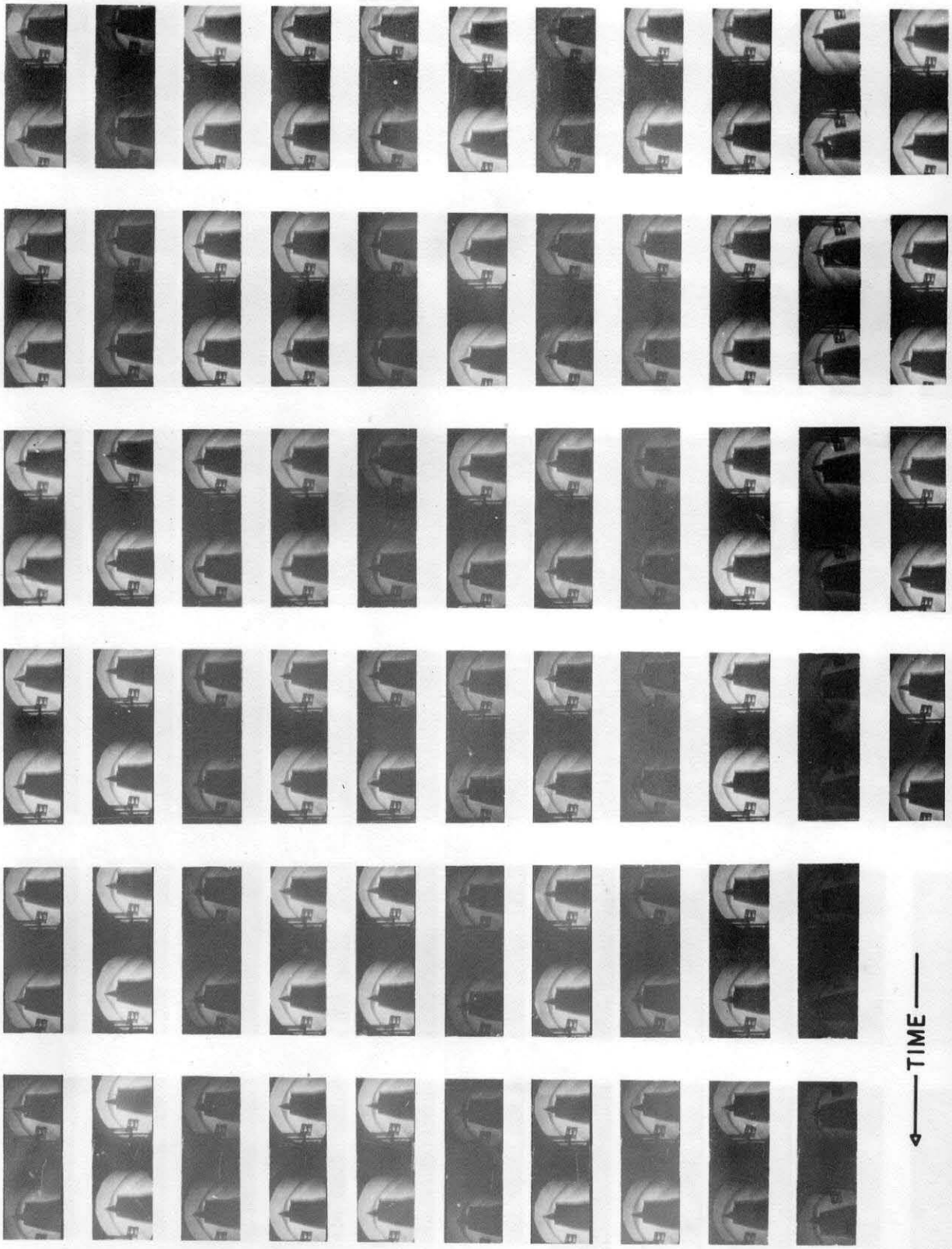

FIG 11(a) ZERO MASS FLOW OSCILLATION
(EFF. LENGTH 6.93 FT.)

FIG 11(b) TYPICAL BUZZ CYCLE NEAR TRANSITION PT.
(6.93 FT.)

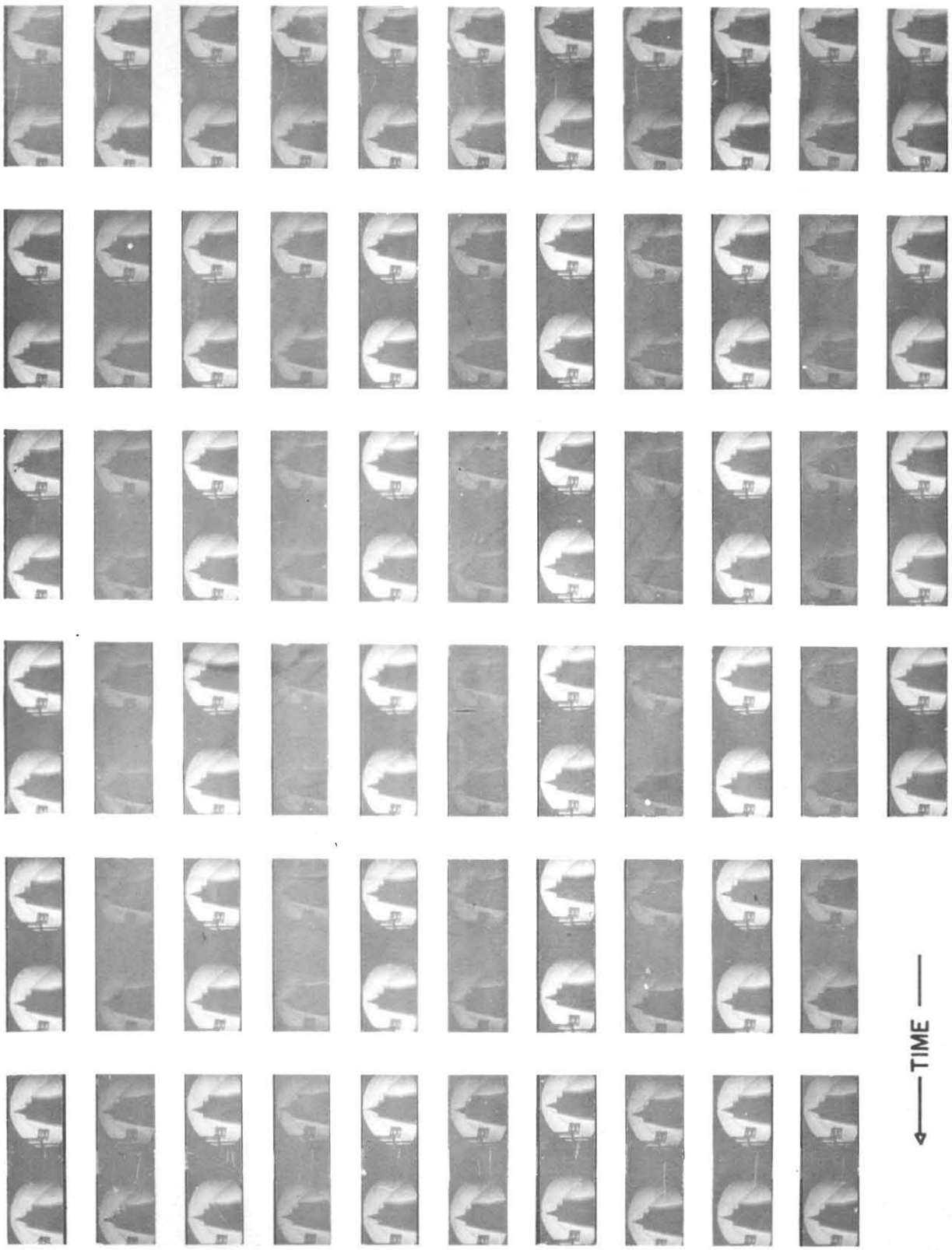

FIG 11(c) RANDOM SHOCK MOTION NEAR CRITICAL PT.
(6.93 FT.)

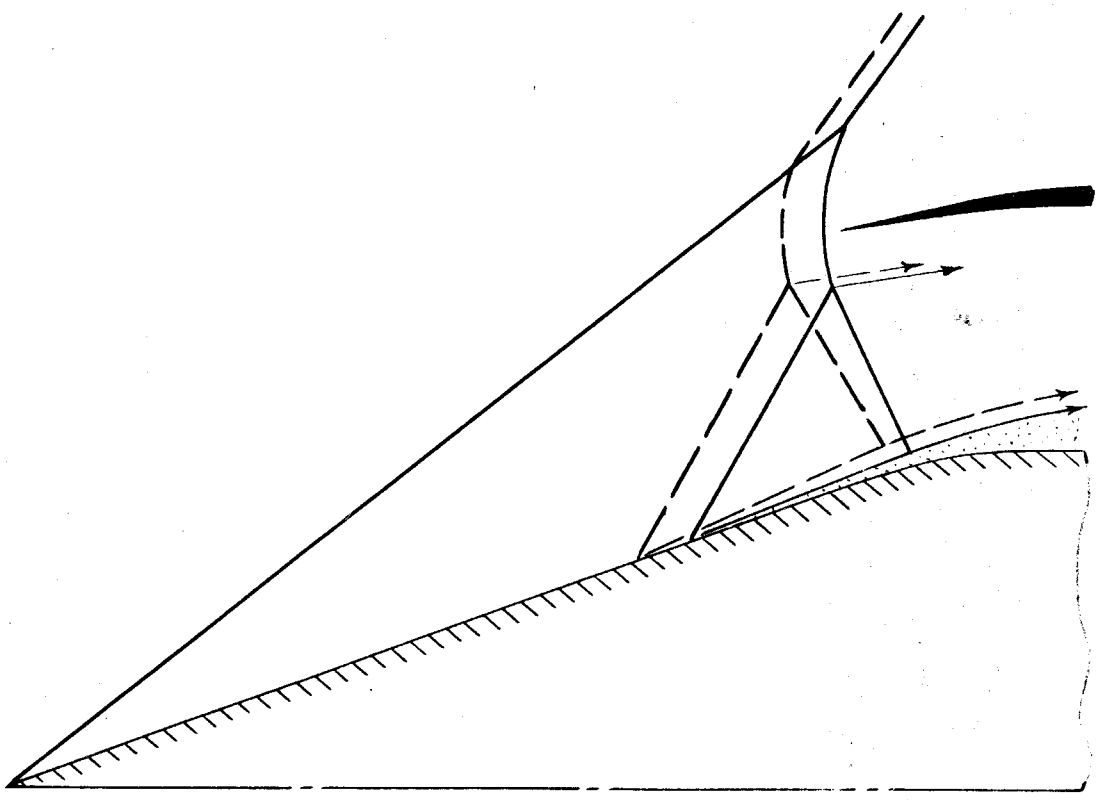

FIG. 12 DECREASED EFFECTIVE INLET AREA DUE TO UPSTREAM MOTION OF SHOCK

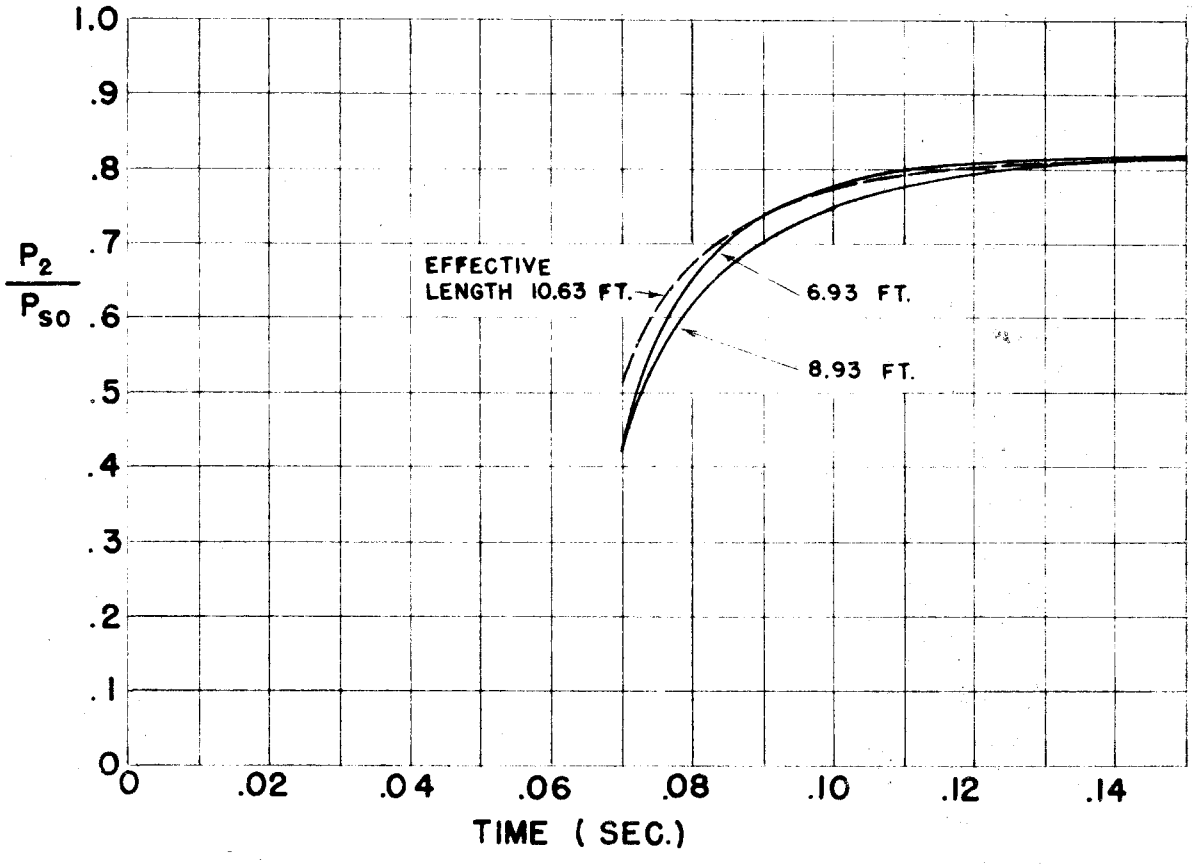

FIG. 13 EFFECT OF PLENUM CHAMBER VOLUME ON CALCULATED FILL-UP TIME

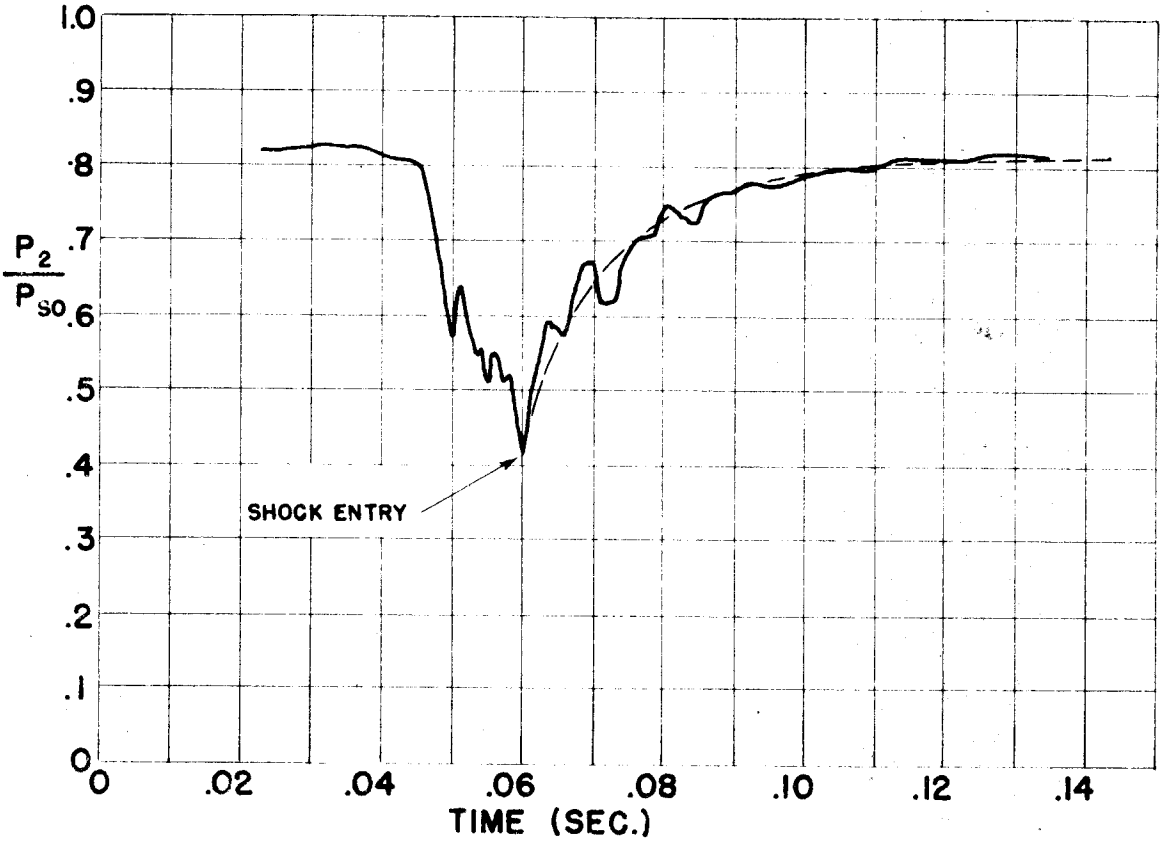

FIG. 14 COMPARISON OF CALCULATED & EXPERIMENTAL FILL-UP TIME (EFFECTIVE LENGTH 6.93 FT.)

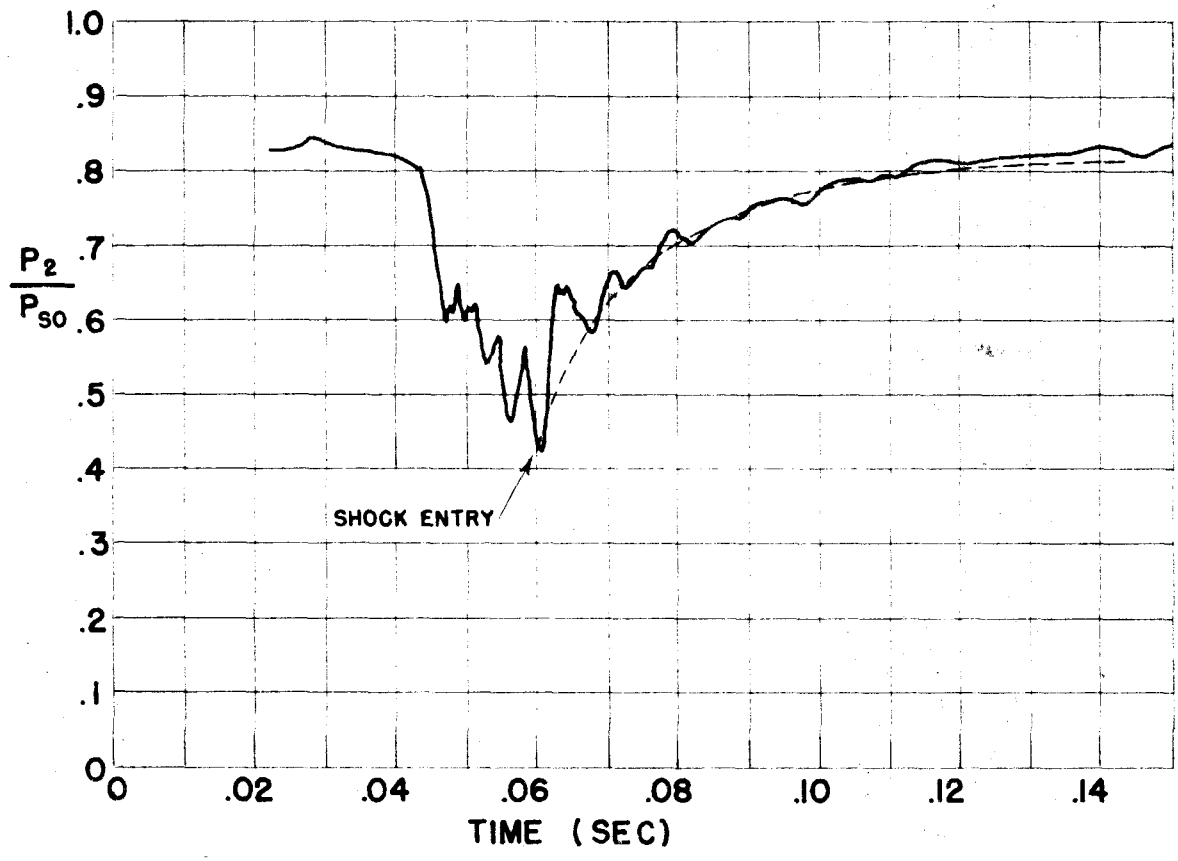

FIG. 15 COMPARISON OF CALCULATED & EXPERIMENTAL FILL-UP TIME (EFFECTIVE LENGTH 8.93 FT.)

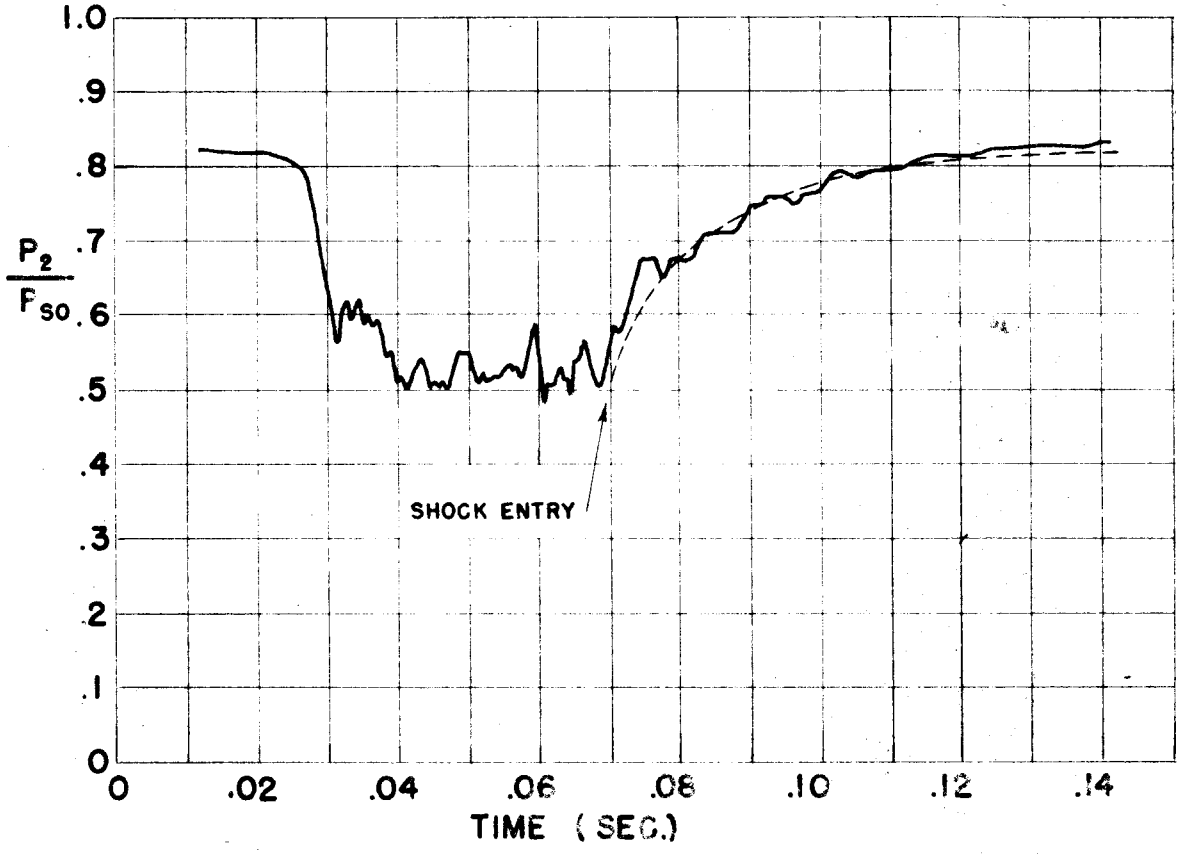

FIG. 16 COMPARISON OF CALCULATED & EXPERIMENTAL FILL-UP TIME (EFFECTIVE LENGTH 10.63 FT.)

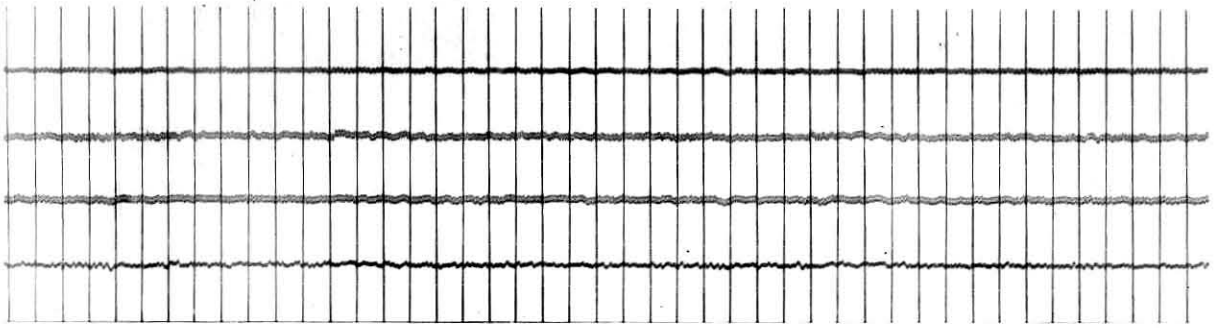

SUPERCRITICAL F/A = 0

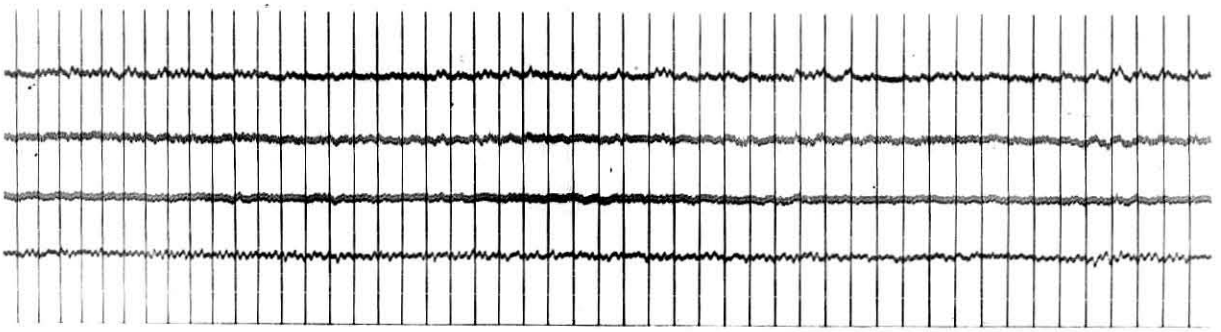

SUPERCRITICAL F/A = .030

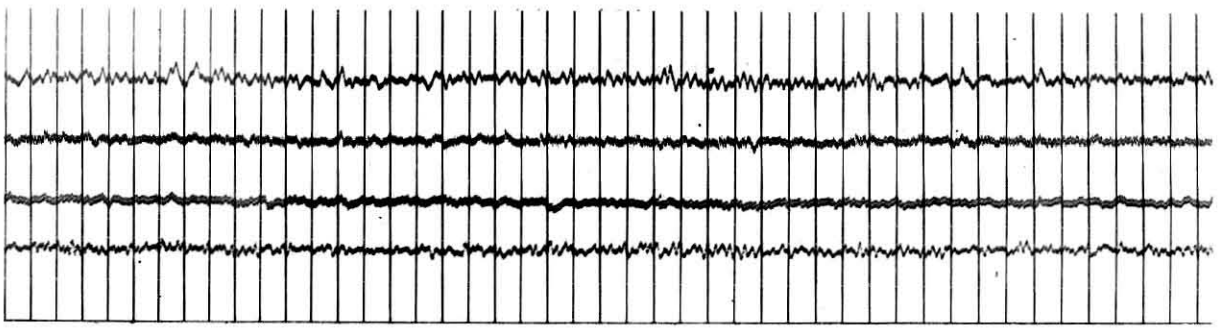

SUPERCRITICAL F/A = .048

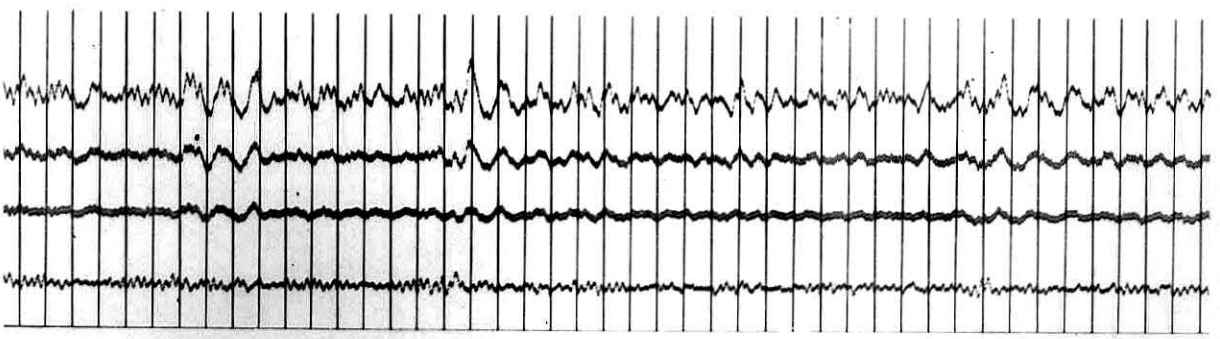

SUPERCRITICAL F/A = .051

FIG. 17 EFFECT OF FUEL AIR RATIO ON BURNING ROUGHNESS

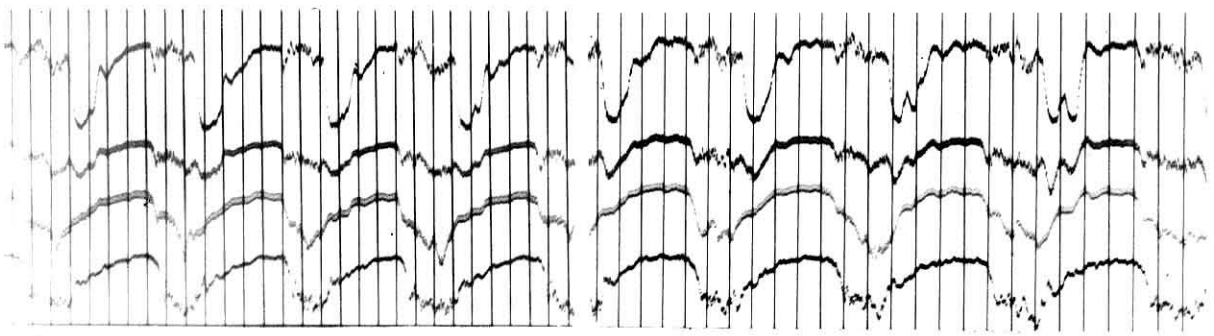

$S_o / S_{oc} = .83$, F/A = 0 $S_o / S_{oc} = .87$, F/A ≠ 0

FIG. 18 EFFECT OF BURNING ON BUZZ CYCLE

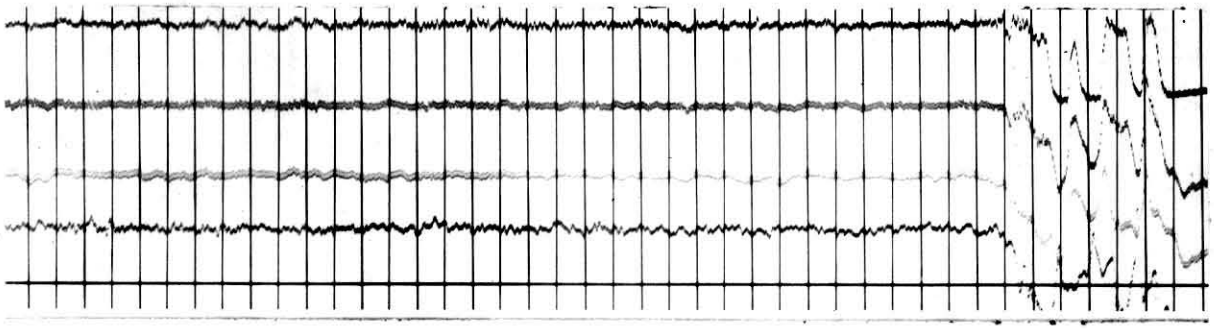

$S_o / S_{oc} = .99$ F/A = .030

FIG. 19 BLOWOUT IN STEADY OPERATION CAUSED BY DIFFUSER INSTABILITY

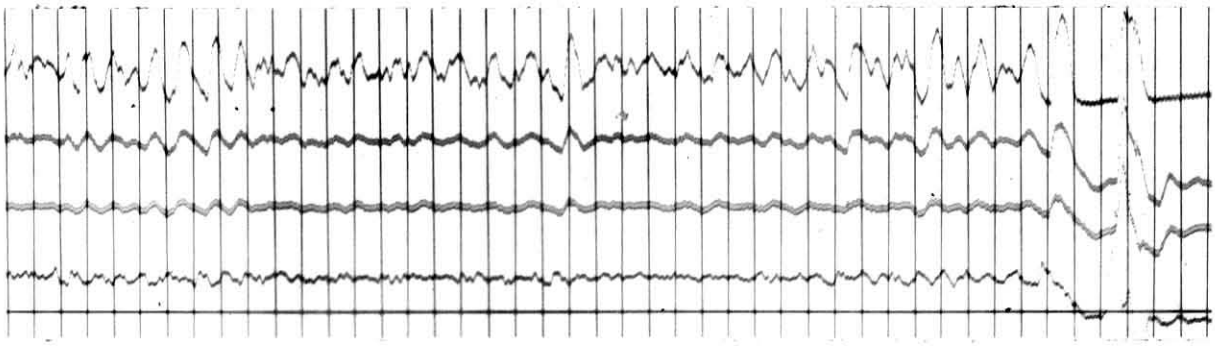

SUPERCRITICAL F/A = .051

FIG. 20 BLOWOUT IN STEADY OPERATION DUE TO ROUGH BURNING

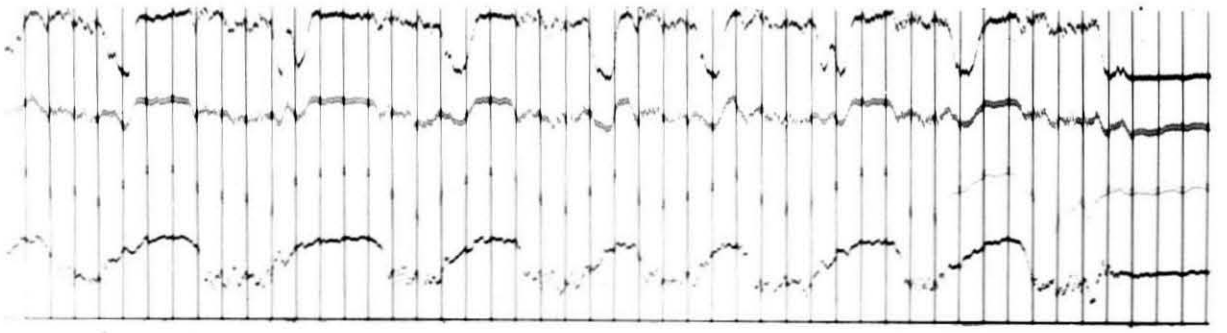

$S_o / S_{oc} = .87$ F/A = .031

FIG. 21 BLOWOUT DURING BUZZ DUE TO BUZZ

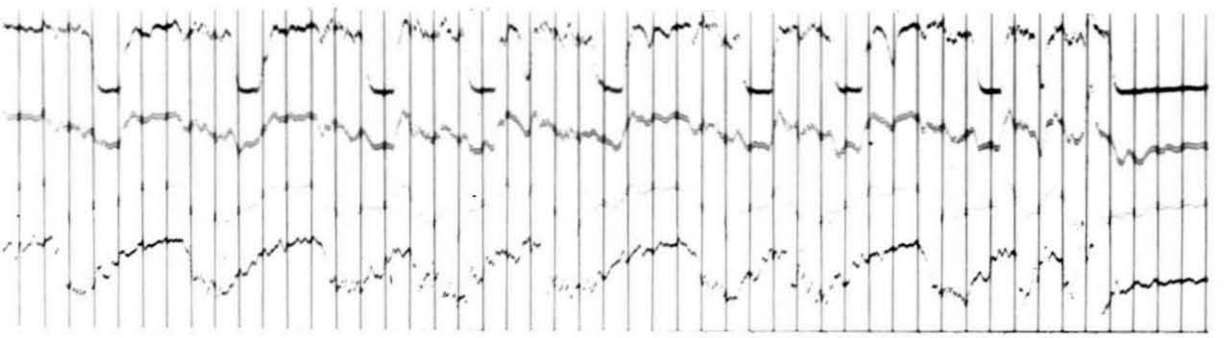

$S_o / S_{oc} = .85$ F/A = .038

FIG. 22 BLOWOUT DURING BUZZ DUE TO ROUGH BURNING